Faculdade de Engenharia da Universidade do Porto
Instituto de Ciências Biomédicas Abel Salazar

NEW MOLECULES AND MECHANISMS ENHANCING AXON GROWTH AFTER SPINAL CORD INJURY

Ana Carolina Sousa Monteiro

Dissertação realizada no âmbito do
Mestrado Integrado em Bioengenharia
Especialização em Biotecnologia Molecular

Orientador: Prof. Dra. Mónica Sousa

Setembro de 2018

"You can't go back and change the beginning, but you can start where you are and change the ending."

C.S. Lewis

Acknowledgements

Chegado o fim desta jornada, resta-me agradecer a todos os que me ajudaram durante este longo percurso e me trouxeram até aqui.

À Mónica, por me ter aceitado como aluna, por toda a disponibilidade e por todos os votos de confiança. À Joana, por toda a paciência e por todo o apoio. À Sara, à Rita e a todos os restantes membros do grupo por toda a ajuda sem entraves.

A todos aqueles que fui encontrando durante estes 5 anos. Aos Cones que entraram comigo e em particular aos 5 de 5 por terem estado lá do início ao fim, nos bons e nos maus momentos. Aos Lindos do ICBAS, quase múltiplos de tudo, por me darem uma casa longe de casa. Aos preferidos que foram aparecendo e que me aturam diariamente sem nunca se queixarem. Ao Tucano y Sus Muchachos, por serem os melhores a construir janelas e a escolher restaurantes, mas principalmente por serem os melhores psciólogos. À Team September por nunca me deixar sozinha nesta luta. A Metal e Bio e a Engenharia, por me terem dado os melhores 5 anos que alguma vez podia ter pedido ao lado de pessoas incríveis, que já são demasiadas para mencionar.

Nunca esquecendo aqueles que já me acompanham há mais de 5 anos e que nunca deixaram de o fazer, às Meninas da Ribeira do Sado e o Zé, por não me deixarem ficar fechada em casa e por estarem sempre prontos para me fazer rir ou para me corrigirem a tese. À Ana e à Rita, por ficarem sempre perto, por muito longe que estejam.

Aos meus pais, por toda a paciência, todo o apoio e toda a liberdade que sempre me deram. Sem eles nada teria sido possível.

A todos o meu mais sincero obrigada.

Abstract

Spinal Cord Injury is a neurological disorder that affects thousands of individuals worldwide each year. Depending on the severity of the injury, different symptoms may appear, namely a partial or total loss of sensory function or motor control in the arms, legs or body. These symptoms are permanent because in the central nervous system axon regeneration fails. This failure is a consequence of the highly inhibitory environment that arises at the injury site, known as the glial scar, and of the intrinsic inability of central neurons to initiate a pro-regenerative program. The main goal of this study was to identify new molecules and new mechanisms that could enhance axon growth or antagonize axon growth inhibition following spinal cord injury. We evaluated the *in vitro* effects of a microtubule-stabilizer drug, ACY-738, to assess its potential to be used as part of a combinatorial therapy for spinal cord injury. Although after one day in culture, the drug caused an inhibition of neurite outgrowth, at day *in vitro* 5 it had a neuroprotective effect on a model of neuronal degeneration. Concordantly, treatment with ACY-738 rescued the dynamic behaviour of degenerating neuronal growth cones. Additionally, using *Acomys cahirinus* as a model for mammal regeneration, we aimed at unraveling the mechanisms that underlie the notable regenerative capacity reported in this species. Here, we report that *Acomys* are able to regain motor and bladder function following complete transection of the spinal cord. This ability is probably associated with reduced fibrosis and the ability of *Acomys* axons to cross the glial scar. Altogether, our results evidence ACY-738 as a New Molecule able to rescue degenerative phenotypes and *Acomys* as a valuable model to unravel New Mechanisms of regeneration in mammals. These findings can constitute the first steps in meeting the major medical need of developing new treatments for spinal cord injury.

Resumo

As lesões da espinal medula constituem uma condição neurológica que afeta milhares de pessoas em todo o mundo. Dependendo da gravidade da lesão, podem aparecer diferentes sintomas, nomeadamente uma perda parcial ou total da função sensorial ou do controlo motor nos braços, pernas ou corpo. Estes sintomas são permanentes porque no sistema nervoso central a regeneração axonal falha, como consequência do ambiente altamente inibitório que surge no local da lesão, conhecido como cicatriz glial, e da incapacidade intrínseca dos neurónios centrais de iniciar um programa pró-regenerativo. O principal objetivo deste estudo foi identificar novas moléculas e novos mecanismos que possam aumentar o crescimento do axónio ou antagonizar a inibição do seu crescimento após uma lesão medular. Avaliámos os efeitos *in vitro* de uma droga estabilizadora de microtúbulos, ACY-738, para perceber qual o seu potencial para ser usada como parte de uma terapia combinatória para lesões medulares. Apesar de depois de um dia em cultura a droga causar uma inibição do crescimento de neurites, após cinco dias *in vitro*, demonstrou um efeito neuroprotector num modelo de neurodegeneração. Concordantemente, o tratamento com ACY-738 resgatou o comportamento dinâmico dos cones de crescimento de neurónios em degeneração. Adicionalmente, usando *Acomys cahirinus* como um modelo da regeneração em mamíferos, procuramos desvendar os mecanismos subjacentes à sua notável capacidade regenerativa. Aqui, relatamos que a espécie *Acomys* é capaz de recuperar a função motora e urinária após uma transecção completa da medula espinal. Esta capacidade está provavelmente associada à fibrose reduzida e à capacidade dos axónios de *Acomys* de atravessar a cicatriz glial. Em conjunto, os nossos resultados evidenciam a droga ACY-738 como uma nova molécula capaz de resgatar fenótipos degenerativos e a espécie *Acomys* como um modelo

valioso para desvendar novos mecanismos de regeneração em mamíferos, e podem constituir os primeiros passos para atender à grande necessidade médica de desenvolver novos tratamentos para lesões na medula espinal.

Contents

List of Figures

efficiently, and produce factors that facilitate Schwann cell migration and axon regeneration. After some time, injured axons form a growth cone and begin to regenerate along a permissive environment formed by Schwann cells. If the axon is able to traverse the injury site, and its environment supports its growth along the entire distal stump, then the axon can connect with peripheral targets. Adapted from [12].

Figure 5. Schematic representation of CNS lesions. In both examples macrophages invade the lesion site and proteoglycans' production by astrocytes is upregulated and a gradient increasing towards the lesion center originates. **A|** Contusive injury does not disrupt the meninges but produces cavitation and proteoglycan deposition. **B|** Stab lesion that penetrates the meninges allows invasion of fibroblasts in addition to macrophages. Abbreviation: ECM – extracellular matrix. Adapted from [16].

Figure 6. Actin and Microtubules Polymerization Dynamics. A| The addition of ATP-actin monomers to the barbed end (+ end) of the actin filament is mediated through profilin and barbed-end-bound elongating factors such as formins. Actin-sequestering proteins like b-thymosin and barbed-end capping proteins like Eps8 limit the polymerization rate. Upon incorporation into the actin filament, hydrolysis of the ATP-actin subunits takes place. ADP-actin monomers or actin filaments fragments are removed from the pointed end (– end) of the filament by the action of depolymerizing or severing factors such as cofilin. Finally, to complete the cycle, the detached actin can exchange its ADP for ATP and be recruited once more to the growing filament barbed end. **B|** For a growing microtubule (left), polymerization occurs most rapidly at the plus (+) end through the addition and removal of α–β-tubulin heterodimers. After incorporation into the microtubule filament, hydrolysis of the β-tubulin-bound GTP takes place. EB proteins can transiently bind to the plus end, influencing polymerization dynamics both directly and indirectly by recruiting other important regulatory +TIPs. For uncapped filaments, slow polymerization and depolymerization can also take place at the microtubule minus (–) end, most likely through similar mechanisms as those occurring at the plus end. Abbreviations: ATP – Adenosine Triphosphate; ADP –

Adenosine Diphosphate; GTP – Guanosine Triphosphate; EB – End-binding; +TIPs – Plus-end Tracking Proteins. Adapted from [28].

Figure 7. Microtubule Dynamics Regulators. Cartoon illustrating how different microtubule-related proteins interact with microtubules. Adapted from [31].

Figure 8. Cytoskeletal Organization in Elongating Axons. The axonal shaft of elongating axons contains stable microtubules whereas their growth cone contains a dynamic cytoskeleton. In the center of growth cones (grey stripped area), dynamic microtubules protrude from the axonal shaft. More peripherally (dark grey area), long bundles of actin radiate outward, giving rise to the filopodia. Meshes of actin filaments, the lamellipodia, intertwine these radial actin bundles. Red and blue arrows represent the main cytoskeletal dynamics leading to axon elongation, respectively for actin and microtubules. Adapted from [37].

Figure 9. Cytoskeletal Organization in Growth Cones versus Retraction Bulbs. A| Growth cones display distinct regions. The center (grey stripped area) contains microtubules which emerge from the axonal shaft. In the periphery (dark grey area) a dense network filaments controls the progression of microtubules towards the axon tip. **B|** In retraction bulbs the separation between different domains is lost. In addition, microtubules are depolymerized to a large extent. The remaining ones are disorganized and do not reach the axon tip. Adapted from [37].

Figure 10. Tubulin Post-Translational Modifications. A| Schematic representation of the α-tubulin-β-tubulin dimer and its associated modifications. **B|** Schematic representation of the generation and removal of α-tubulin acetylation. **C|** Localization of tubulin PTMs. Acetylation of α-tubulin Lys40 is exposed to the luminal face of microtubules. All modifications are shown using the color code detailed in part A. Abbreviations: αTAT1 - α-tubulin N-acetyltransferase 1; HDAC6 - Histone

Deacetylase 6; SIRT2 - Sirtuin 2; PTM – Post-Translational Modifications; Lys40 - Lysine Residue 40. Adapted from [50].

Figure 11. Wild-type versus Twitcher Mouse. Lose weight and a hunched back are characteristic of the twitcher mouse. 42-day old littermates: Upper mouse, wild-type; lower mouse, twitcher. Adapted from [78].

Figure 12. Kymographs for Microtubule Growth Speed Quantification. Kymographs obtained with ImageJ plugin KymoResliceWide. The original kymograph (**A**|) was modified by changing the lookup table, obtaining a better visualization of the existing comets in the modified kymograph (**B|**). Only comets with three or more steps were considered: upper comet was excluded, lower comet was included.

Figure 13. Digestion Patterns of Genomic PCR Fragments. Following restriction digestion, an upper band defines a non-mutated allele and a lower band defines a mutated allele. Therefore, a single upper band defines the mouse as a WT and one lower band defines it as an affected twitcher mouse. If two bands are present, then the mouse is heterozygous. Abbreviations: Het – Heterozygous; WT – Wild Type; twi – twitcher.

Figure 14 - Neurite Outgrowth of DRG Neurons: DIV1. A| Total neurite length. Treatment with ACY-738 reduces the total neurite length of both WT and twitcher neurons. **B| Sholl Analysis.** Treatment with ACY-738 reduces the branching of both WT and twitcher neurons. **C| Representative Images of DRG Neurons.** Scale bars: 100 μm. Abbreviations: WT – Wild Type; DMSO – Dimethyl sulfoxide; DRG – Dorsal Root Ganglia.

Figure 15 - Neurite Outgrowth of DRG Neurons: DIV5. A| Total neurite length. Treatment with ACY-738 reduces the total neurite length of WT neurons and shows a tendency to increase neurite outgrowth in twitcher neurons. **B| Sholl Analysis.** At DIV5, branching is reduced in all conditions. Treatment with ACY-738 reduces branching in WT but not in

twitcher neurons. **C| Representative Images of DRG Neurons.** In order to get a better perception of individual cells, SynD Neurite Masks are presented instead of the original images. Scale bars: 100 μm. Abbreviations: WT – Wild Type; DMSO – Dimethyl sulfoxide; DRG – Dorsal Root Ganglia.

Figure 16 - Microtubule Growth Speed. A| Axon Shaft. In the axon shaft, treatment with ACY-738 reduces the microtubule growth speed of both WT and twitcher DRG neurons. **B| Growth Cone.** In growth cones, ACY-738 causes a decrease of both WT and twitcher neurons microtubule growth speed.

Figure 17 - *Acomys* present skin autotomy and subsequent rapid healing. The same wounds in **A|** are no longer visible at D30 and new spiny hairs cover the damaged area (**B|**). Adapted from [91].

Figure 18 - Ear punch closure of *Acomys cahirinus*. A| Timeline of ear punch closure of *Acomys cahirinus* versus *Mus* C57BL/6 at weekly intervals between day 14 and day 56. Scale bar 1 mm. **B-I|** Immunofluorescence analysis of regenerated *Acomys cahirinus* ear punch. B| Incubated with anti-actin (50x). C| Probed with anti-actin (200×). D| Negative control in which the primary antiserum was omitted (200×). E| Incubated with anti-TUJ1 (50x). F| Probed with anti-TUJ1 (200×). G| Negative control stained with secondary antibody only (200×). H| Merge of B+E+Dapi (5x). I| Merge of B+E+Dapi (200×). All scale bars 100 μm. Adapted from [92].

Figure 19 – Immunostaining for the extracellular matrix proteins reveals differences in the total area of protein deposition. A, C, E| Representative images for immunohistochemistry to detect collagen I (A|), fibronectin (C|) and tenascin (E|) in *Mus musculus* and *Acomys cahirinus*. Scale bar, 100 μm. **B, D, F|** To quantify positive signal, a region of interest was created to include tissue distal to the original cartilage and to exclude hair follicles and epidermis. The ratio of total immuno-positive area per total area of the region of interest was calculated. Data represent mean and s.e.m., *t-test $p<0.05$ for *Mus musculus* versus *Acomys cahirinus*

comparison for the day indicated. Abbreviations: Col1 – collagen I; FN – fibronectin; TNC – tenascin; RBC – red blood cells. Adapted from [93].

Figure 20 – *Acomys* display functional recovery following spinal cord injury. A| BMS Score. After complete transection of the spinal cord, *Acomys* recover some locomotor function. **B| Bladder Function.** *Acomys* are able to regain bladder control following injury. *Mus* do not recover motor or bladder control. Abbreviations: BMS – Basso Mouse Scale; SCI – Spinal Cord Injury.

Figure 21 - DRG neurons from *Acomys* have an increased axon growth capacity *in vitro*. *Acomys* DRG neurons have an increased total neurite length (**A|**) and branching (**B|**) under permissive and inhibitory environments when compared with *Mus*.

Figure 22 - Histological spinal cord section of *Acomys* labelled for GFAP. Similar to *Mus*, after injury, *Acomys* spinal cord presents increased expression of GFAP with local astrocyte activation. Scale bar 500 μm. Abbreviations: GFAP – Glial Fibrillary Acidic Protein; R – Rostral; C – Caudal.

Figure 23 - Histological spinal cord section of *Acomys* labelled for Cholera Toxin Subunit B. CTb-labelled ascending axons are not able to regenerate rostrally to the lesion site. Scale bars: 500 μm. Abbreviations: R – rostral; C – caudal.

Figure 24 - Histological spinal cord sections of *Acomys* and *Mus* stained with Masson's Trichrome staining. *Acomys* spinal cord exhibits lower collagen deposition, indicating a reduced fibrosis, when compared with *Mus* in which collagen is accumulated at higher levels (fibrotic scarring) at 12 weeks after injury. Scale bar: 500 μm. Abbreviations: R – Rostral; C – Caudal.

Figure 25 - *Acomys* descending serotonergic axons have the ability to cross the glial scar following injury. Serotonin staining is observed caudally (**B|**) to the lesion site. Scale bar = 500μm.

Figure 26 – Histological spinal cord sections of *Acomys* labelled for βIII-tubulin and SCG10. A| βIII-tubulin. There are no visible axons crossing the lesion site. **B| SCG10.** There are regenerating axons on both sides of the lesion (white arrows, **C|** and **D|**). Scale bars: 500 μm. Abbreviations: R – Rostral; C – Caudal.

Figure 27 – Histological spinal cord section of *Acomys* labelled for Collagen I. After injury, *Acomys* spinal cord presents increased expression of collagen in the lesion site. Scale bar 500 μm. Abbreviations: R – Rostral; C – Caudal.

Figure 28 –Histological spinal cord section of *Acomys* labelled for IBA1. A| 10x objective. IBA1 efficiently stained the spinal cord section. Scale bar: 500 μm. **B| 20x objective.** Using a higher magnification it is possible to visualize "star" shaped cells, indicated by the white arrows. Scale bar: 100 μm. Abbreviations: R – Rostral; C – Caudal.

Figure 29 – Locomotor Function Recovery in *Acomys*. Representative frames of open field locomotion videos. **A| 2 days post-injury.** Absence of ankle movement, BMS score 0. **B| 5 weeks post-injury.** Weight supported plantar stepping, BMS score 4.

List of Tables

Abbreviations

+TIP	Plus-End Tracking Proteins
5-HT	5-hydroxytryptamine
ADP	Adenosine Diphosphate
ATP	Adenosine Triphosphate
BMS	Basso Mouse Scale
bp	Base Pairs
BSA	Bovine Serum Albumin
CNS	Central Nervous System
CO_2	Carbon Dioxide
CSPG	Chondroitin Sulphate Proteoglycan
CTb	Cholera Toxin Subunit B
DAPI	4',6-diamidino-2-phenylindole, dihydrochloride
DIV	Days *in vitro*
DMEM	Dulbecco's Modified Eagle Medium
DMSO	Dimethyl Sulfoxide
DRG	Dorsal Root Ganglia
EB	End-Binding
ECM	Extracellular Matrix
FBS	Fetal Bovine Serum
GALC	Galactosylceramidase
Gal-Cer	Galactosylceramide
GDP	Guanosine Diphosphate
GFAP	Glial Fibrillary Acidic Protein
GFP	Green Fluorescent Protein
GLD	Globoid Cell Leukodystrophy
GTP	Guanosine Triphosphate
HDAC	Histone Deacetylase
IC_{50}	Half Maximal Inhibitory Concentration
IHC	Immunohistochemistry
L-Glu	L-Glutamine
MAI	Myelin-Associated Inhibitor
MAP	Microtubule-Associated Protein
MT	Microtubule
NGF	Nerve Growth Factor

NH_4Cl	Ammonium Chloride
O/N	Overnight
P/S	Penicillin-Streptomycin
PB	Phosphate Buffer
PBS	Phosphate-Buffered Saline
PFA	Paraformaldehyde
PLL	Poly-L-Lysine
PMA	Phosphomolybdic Acid
PNS	Periferal Nervous System
PTA	Phosphotungstic Acid
PTM	Post-Translational Modification
RT	Room Temperature
SCI	Spinal Cord Injury
SEM	Standard Error of the Mean
SIRT2	Sirtuin 2
SynD	Synapse Detector
TBS-T	Tris-Buffered Saline - 1% Triton X-100
WT	Wild-type
α-TAT1	α-tubulin N-acetyltransferase

Chapter 1

Context and Motivation

According to the World Health Organization fact sheet on Spinal Cord Injury [1], every year about 250 000 to 500 000 people around the world suffer a spinal cord injury (SCI), which refers to any damage to the spinal cord, resulting from trauma, degeneration or disease.

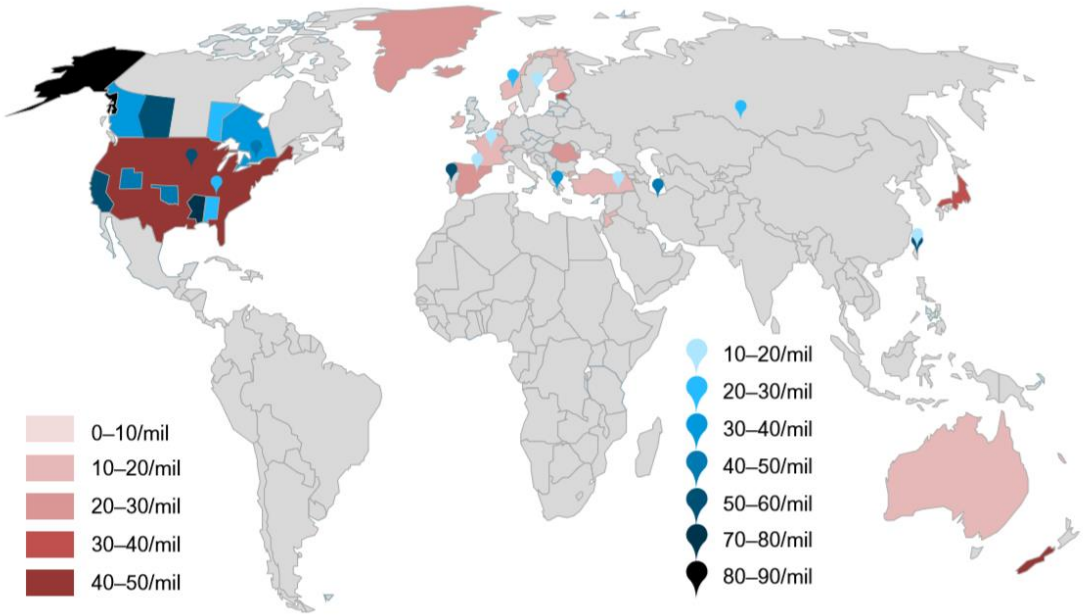

Figure 1 - Relative annual incidences of traumatic spinal cord injury worldwide. The red color scheme refers to national data, while the blue color scheme refers to states, provinces or regions. Abbreviation: mil – million. Adapted from [2].

In 2014, Singh et al. systematically reviewed the literature reporting either the incidence (number of new cases in a given period of time) or the

prevalence (proportion of a population living with the disability at a particular time) of SCI worldwide [2]. A world map representing the relative incidences at a national or regional level, from 1959 until 2011, is shown on Figure 1. Moreover, more recent data regarding the incidence and prevalence of this disability in the United States of America indicates that there are about 17 700 new cases per year, which translates into 54 new cases per million, and an estimate 288 000 people currently affected [3]. Given these numbers, it is possible to understand that SCI affects not only the well-being of affected people, but also places a great financial burden on the health care systems.

Even though the proportion of non-traumatic injuries appears to be increasing, most cases of SCI are still due to traumatic causes [1], such as falls, motor vehicle accidents or crashes, sports-related accidents or violence, including gunshots or stabbing. As well as its incidence and prevalence, SCI causation also differs when comparing developed and developing countries. A global perspective on the traumatic causes is shown on Figure 2.

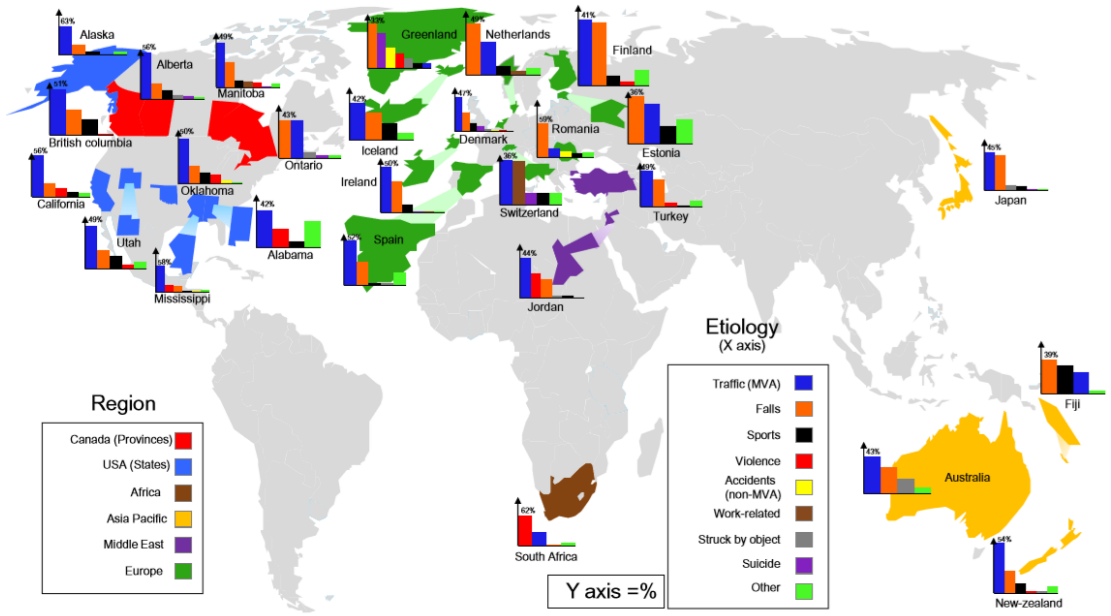

Figure 2 - Spinal cord injury causations in different countries. In the bar graphs, the x-axis categorizes the reported causes, while the y-axis indicates their percentage of contribution. Abbreviation: MVA - motor vehicle accident. Adapted from [2].

Depending on the severity of the injury and its location on the spinal cord, different symptoms may appear. Most people experience chronic pain, and there may be a partial or total loss of sensory function or motor control in the arms, legs or body. In the most severe cases, the systems that regulate bowel or bladder control, breathing, heart rate and blood pressure are affected [1].

Spinal cord injuries may result in the development of secondary conditions that are debilitating and may become life-threatening and, therefore, there is a need for their prevention and management.

Currently, the measures for improving the health of people with spinal cord injury include acute care (including surgical procedures of stabilization and decompression of the spinal cord), rehabilitation services and ongoing health maintenance, in order to prevent further injury and empower people with an SCI to return to an active life [1]. However, there are still no known ways to reverse damage to the spinal cord and there is a continuous research on new possible treatments which may promote regeneration of cells after injury, including cell therapy, molecular therapy or combinatorial therapies. Although some studies have shown modest benefits, there are still no fully restorative treatments and, therefore, there is a major need to identify new strategies to repair the injured spinal cord [4], and that is the fundamental goal of the work developed on this thesis.

Chapter 2

Introduction

Regeneration in the Nervous System

The nervous system is a complex network of highly specialized cells that transmit signals between different parts of the body. This system has several levels of organization, starting with two main parts: the peripheral nervous system (PNS) and the central nervous system (CNS). The spinal cord, together with the brain, forms the central nervous system (CNS), which is the control center responsible for processing sensory input. The transmission of motor commands in response to this sensory information is the function of the peripheral nervous system (PNS), formed by nerves and ganglia.

The main cells that constitute the nervous system, the neurons, are capable of rapidly transferring information from one part of the body to another, since they form different tracts within the spinal cord, along which the impulses travel. These tracts, which establish the communication between the brain and the spinal cord, can be ascending or descending (Figure 3), being respectively sensory, delivering information to the brain, or motor, delivering information to the periphery and causing the body to respond in a variety of ways [5].

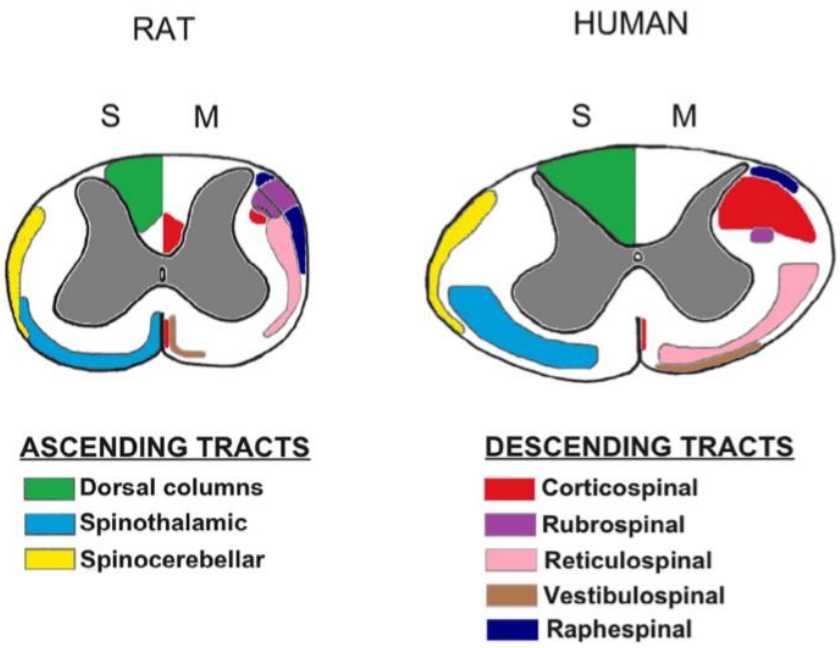

Figure 3 - Comparative anatomy of the rat and human spinal cords. The grey matter of the spinal cord is surrounded by white matter through which spinal cord tracts run longitudinally. Approximated location of ascending and descending tracts in each species is represented. Abbreviations: S – sensory tracts; M – motor tracts. Adapted from [4].

Neurons are remarkable due to their ability of effectively and rapidly responding to several types of cell signaling, integrating and regulating the information in order to transmit it over long distances by electrical impulses. These cells are constituted by a cell body (or soma) and neuronal processes called neurites, which may become dendrites or axons, and allow the generation of a functional neuronal network: the dendrites receive signals from body tissues or other neurons and pass them into the cell body. When an output signal is produced, it goes down the axon and passes to the next neuron or to the target cell.

However, neurons account for only a small part of the nervous tissue, since they are surrounded and protected by glial cells, or neuroglia. These are non-neuronal cells that maintain homeostasis, form myelin, provide support, nutrition and insulation for neurons, and help with signal transmission. In the PNS, glial cells include Schwann cells and satellite cells, while in the CNS these include oligodendrocytes, astrocytes, ependymal cells and microglia. Schwann cells and oligodendrocytes are responsible for the myelination of PNS and CNS axons, respectively. The formation of a

multilayered myelin sheath electrically insulates axons, thus limiting the generation of action potentials to myelin-free regions of axons, the nodes of Ranvier, allowing a fast propagation of the electric impulses through the nerves [6].

Due to its vital role in maintaining internal order within the body, when the nervous system is injured, if regeneration of the damaged tissue in order to restore its function does not occur, permanent cognitive or sensorimotor disabilities may arise. It has been recognized that axon regeneration is the only way to restore function after severe spinal cord injuries that interrupt the long tracts that mediate motor and sensory function and, as such, control of central axon regeneration is a major unmet medical need.

This regenerative process can be viewed as an attempt to recapitulate the developmental process. During development, neural progenitor cells divide asymmetrically, giving rise to a daughter progenitor cell and to a neuron. That unpolarized neuron starts migrating to its target and along that process becomes polarized, originating an axon and dendrites [7]. Both the axon formation and its elongation are strongly dependent on cytoskeleton dynamics, since actin destabilization [8] and microtubules stabilization [9] are essential for these processes. Axonal elongation declines throughout the developmental process, given the loss of neuronal intrinsic ability to elongate and correctly reach their post-synaptic targets [10] and, therefore, for a long time the nervous system was thought to be unalterable after maturation.

The first descriptions of axonal regeneration were made in 1928, when Ramon y Cajal described the peripheral nervous system as a supportive environment that could orient the regrowth of injured axons. On the other side, axons in the central nervous system were described as incapable to regrow, because the axons formed swellings at the tip in the lesion site, which were designated as retraction bulbs [11]. While these bulbs lack a regenerative response, in axons which are able to regenerate there is the formation of a growth cone at their transected tip; growth cones and retraction bulbs will be further described in Chapter 3.

Despite all of the scientific advances and the discovery of many mechanisms underlying axonal growth, the general understanding in the

axonal regeneration field has not changed much since these first descriptions and, therefore, new studies that allow a better understanding of these processes and the development of new strategies to promote CNS axon regeneration are immensely significant.

Regeneration is Possible: The Peripheral Nervous System

Following injury to the PNS, both motor and sensory axons are able to spontaneously regenerate and regrow to a significant extent.

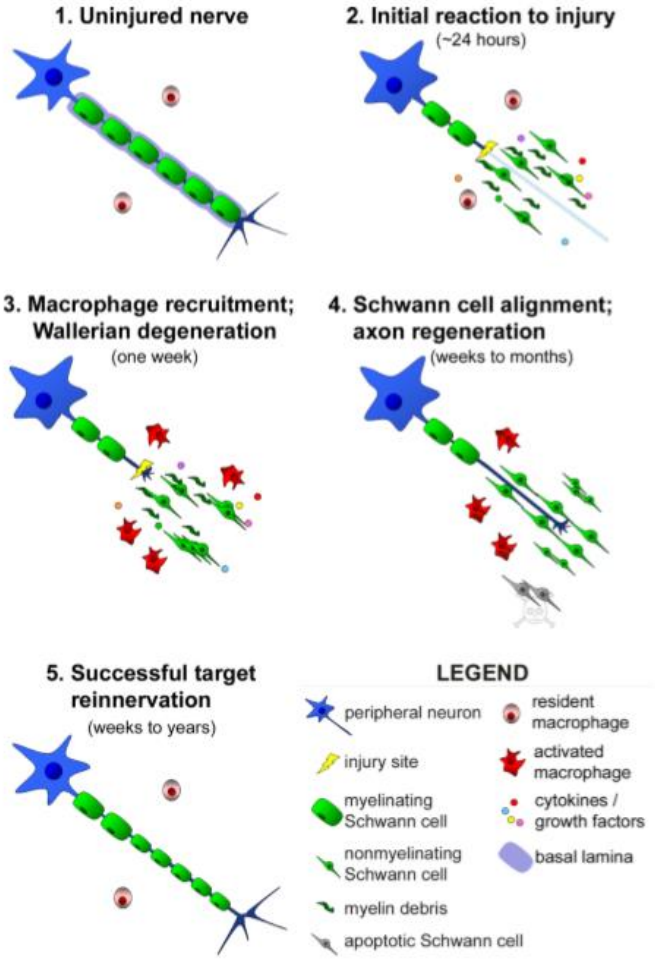

Figure 4 - Progression of Wallerian degeneration and axon regeneration after peripheral nerve injury. Soon after injury, denervated myelinating Schwann cells release their myelin and then start to proliferate, producing cytokines and trophic factors, and phagocytosing detached debris. Soluble factors produced by Schwann cells and injured axons activate resident macrophages, which clear myelin and axon debris efficiently, and produce factors that facilitate Schwann cell migration and axon regeneration. After some time, injured axons form a growth cone and begin to regenerate along a permissive environment formed by Schwann cells. If the axon is able to traverse the injury site, and its environment supports its growth along the entire distal stump, then the axon can connect with peripheral targets. Adapted from [12].

The process which allows axonal regeneration in the PNS is Wallerian Degeneration, a response from non-neuronal cells to injury.

The key event in this process is the degeneration of the disconnected distal portion of the axons, which triggers a cascade of responses by Schwann cells and macrophages that eventually lead to the clearing of the inhibitory debris, as well to a production of a growth-permissive environment [12]. The progression of Wallerian Degeneration is described in Figure 4.

Why is the CNS unable to regenerate?

While PNS axons readily regenerate, allowing recovery of function after peripheral nerve damage, CNS axons do not have the ability to spontaneously do so. The main question is why the CNS is unable to regenerate. When Ramon y Cajal first described dystrophic endballs in CNS axons, these structures were thought to no longer be capable of regeneration [11]. This suggested that regeneration failure could be attributed to the decline in the intrinsic growth ability of neurons that occurs along the development. However, early studies by Aguayo et al. have shown that severed axons are able to preserve a restricted capacity for regrowth, as they are able to extend over long distances when provided with a peripheral nerve graft as growth environment [13]. In this way, it is evidenced that the extrinsic environment present in CNS lesions is also an important factor to understand the inability of this system to regenerate.

Throughout the years, many components of the inhibitory environment of the CNS have been identified. The two major classes of axon regeneration inhibitors are the myelin-associated inhibitors (MAIs) and the chondroitin sulphated proteoglycans (CSPGs) [14].

MAIs are expressed by oligodendrocytes as components of CNS myelin. As the myelin structure that ensheaths axons may be damaged after injury, lesioned axons may be exposed to these components, given that oligodendrocytes and microglia lack phagocytic properties to clean the debris [12], as Schwann cells do in the PNS during Wallerian degeneration. CNS myelin was defined as a source of inhibition when it was found to inhibit axon outgrowth *in vitro*, unlike PNS myelin [15].

CSPGs are inhibitory extracellular matrix (ECM) molecules present in the cellular and molecular barrier formed upon injury, known as the glial scar.

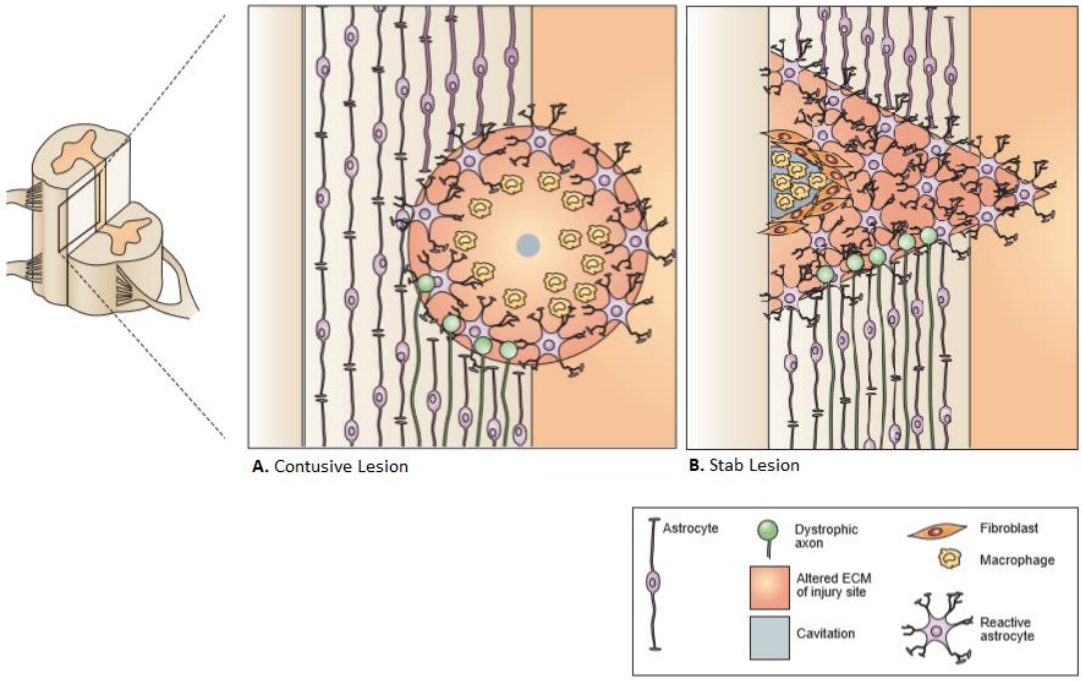

Figure 5 - Schematic representation of CNS lesions. In both examples macrophages invade the lesion site and proteoglycans' production by astrocytes is upregulated and a gradient increasing towards the lesion center originates. **A |** Contusive injury does not disrupt the meninges but produces cavitation and proteoglycan deposition. **B |** Stab lesion that penetrates the meninges allows invasion of fibroblasts in addition to macrophages. Abbreviation: ECM – extracellular matrix. Adapted from [16].

The constitution of this scar depends on the severity of the injury, as depicted in Figure 5, but there is always an abundance of reactive astrocytes. One of the major elements of this reactive glial response to injury is hypertrophy, with increased expression of intermediate filaments [16], which allows the identification of reactive astrocytes by immunocytochemical methods, staining for glial fibrillary acidic protein (GFAP), the major protein present in these filaments [17].

While there are a lot of beneficial effects that arise from reactive astrocytes' response, since the formation of the glial scar isolates the injury site and, therefore, minimizes the inflammatory response and the cellular degeneration [14, 16], it is also this response that originates the excess of CSPGs, since these are released by hypertrophic astrocytes [18]. CSPGs are

proteoglycans, that is, they are constituted by a protein core linked to highly sulphated glycosaminoglycan chains, which consist of repeating disaccharide units. These molecules form a rather large family, which includes aggrecan, versican, brevican, neurocan, phosphacan and NG2 [19]. It has been shown that CSPG expression is highly upregulated in the glial scar of animals, originating an inhibitory gradient, which gradually increases from the periphery until the center of the lesion [16, 20]. Several studies have demonstrated the inhibitory effect of CSPGs on axon outgrowth *in vitro* [21, 22].

Despite the great influence that the extrinsic environment at the lesion site has on the failure of axon regeneration in the CNS, it has been shown that blocking extracellular cues alone is not sufficient to allow complete regeneration [23]. This finding emphasizes the need for a better understanding of the intrinsic mechanisms that may control the regenerative capacity of neurons.

Indeed, CNS neurons are not able to mount a robust pro-regenerative program and recapitulate developmental pathways unlike PNS neurons [14]. This incapacity has been related with low calcium changes at the time of the injury: calcium influx into the axoplasm is one of the first signals that a lesion has occurred and it elicits several mechanisms that contribute to the successful axon regrowth. Therefore, lower amplitudes in calcium changes in CNS neurons [24] can compromise the regenerative process. Besides decreased calcium changes, CNS neurons present a decreased expression of regeneration-associated genes (RAGs) when compared to PNS neurons [14, 25].

Regardless of this inability to regenerate, regrowth of CNS axons may be activated under specific conditions, such as the ones elicited by a conditioning lesion. Dorsal root ganglia (DRG) neurons possess two axonal branches: one peripheral, which regenerates upon injury, and one central that does not. However, if the peripheral branch is lesioned prior to the central branch, the so-called conditioning lesion, the central axon is able to regenerate to significant extents, both *in vitro* and *in vivo* [26]. This conditioning effect is likely caused by the activation of regenerative machinery before the occurrence of the central lesion. Since the central axons of DRG neurons share the same inhibitory environment as axons of

the spinal cord, it is thought that the molecular mechanisms controlling axon regeneration in the central branch of DRG neurons can be the key to uncover new ways to enhance CNS axon regeneration. For this reason, adult DRG neurons are widely used as a model system to study regenerative axon growth.

Objectives

The basis of this thesis is the CNS inability to regenerate and the main goal is to identify new molecules and new mechanisms that may promote axon regeneration after spinal cord injury.

In Chapter 3 the focus is on "**New Molecules**", as we evaluated the *in vitro* effects of a microtubule-stabilizer drug and its potential to be used as part of a therapy for SCI.

Chapter 4 on its turn will be around "**New Mechanisms**" as we explored spinal cord regeneration in *Acomys cahirinus*, a mammal with high regenerative capacity, aiming to provide valuable insights into the spinal cord regeneration field.

Chapter 3

ACY-738: A Specific Inhibitor of a Microtubule Associated Deacetylase

I. Theoretical Background

Central neurons are unable to start a pro-regenerative program after injury since they lose their intrinsic growth ability upon maturation. A variety of processes gives rise to this intrinsic inhibition. Among them, pathological cytoskeleton dynamics have emerged as a major obstacle to regeneration. Understanding this processes and how to modulate them may be the key to find a powerful and potentially clinically translatable strategy to enhance regeneration after spinal cord injury.

Dynamic Instability of the Cytoskeleton

During nervous system development, maintenance and regenerative processes, there is a need of a well-organized machinery that shuttles vital cellular components from the cell body along the axon.

The cytoskeleton is a complex network of polymeric filaments and regulatory proteins, which provide structure and support to cells and their cytoplasmic constituents. The three major components of this system are actin microfilaments, intermediate filaments and microtubules (MT) [6]. These different filaments are distinguishable by their mechanical rigidity, polarity, associated molecular motors and dynamics of assembly [27].

Contrary to what the name "skeleton" suggests, the cytoskeleton is a highly dynamic system in which fibers are constantly degraded and renewed, under tight regulation. Actin filaments and MT are central to this dynamic action of the cytoskeleton, particularly in highly motile areas, such as the axonal growth cone [28]. As both actin and MT are formed by asymmetrical subunits, the filaments are polarized and their polymerization occurs mainly at one end – the barbed end of actin and the plus end of microtubules [28]. Polymerization dynamics are further described in Figure 6.

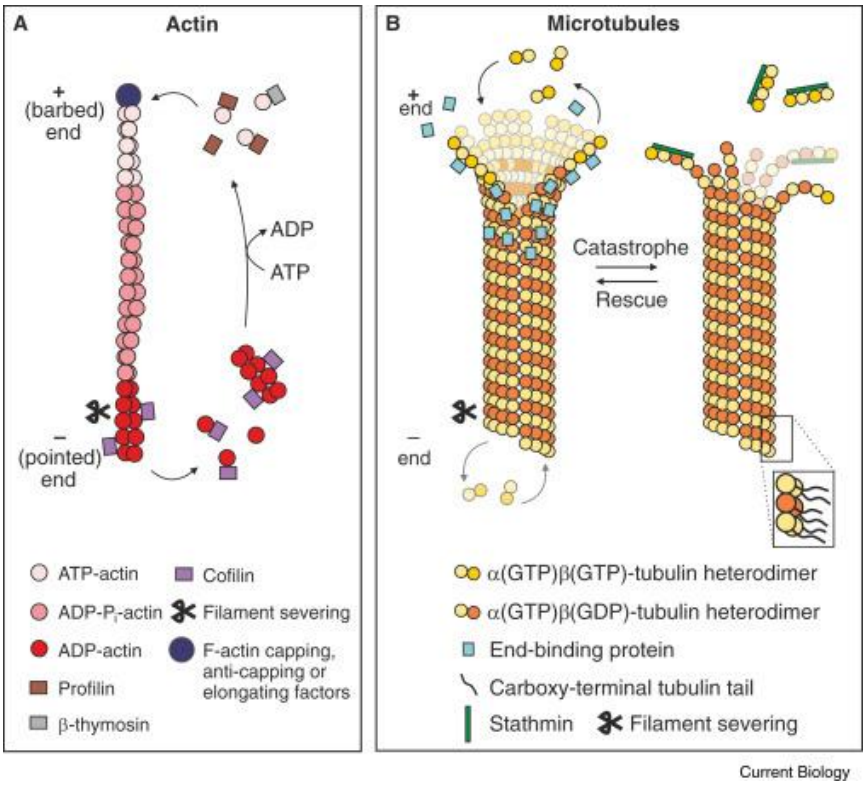

Figure 6 - Actin and Microtubule Polymerization Dynamics. A| The addition of ATP-actin monomers to the barbed end (+ end) of the actin filament is mediated through profilin and barbed-end-bound elongating factors such as formins. Actin-sequestering proteins like b-thymosin and barbed-end capping proteins like Eps8 limit the polymerization rate. Upon incorporation into the actin filament, hydrolysis of the ATP-actin subunits takes place. ADP-actin monomers or actin filament fragments are removed from the pointed end (- end) of the filament by the action of depolymerizing or severing factors such as cofilin. Finally, to complete the cycle, the detached actin can exchange its ADP for ATP and be recruited once more to the growing filament barbed end. **B|** For a growing microtubule (left), polymerization occurs most rapidly at the plus (+) end through the addition and removal of α-ß-tubulin heterodimers. After incorporation into the microtubule filament, hydrolysis of the ß-tubulin-bound GTP takes place. EB proteins can transiently bind to the plus end, influencing polymerization dynamics both directly and indirectly by recruiting other important regulatory +TIPs. For uncapped filaments, slow polymerization and depolymerization can also take place at the microtubule minus (-) end, most likely through similar mechanisms as those occurring at the plus end. Abbreviations: ATP – Adenosine Triphosphate; ADP – Adenosine Diphosphate; GTP – Guanosine Triphosphate; EB – End-binding; +TIPs – Plus-end Tracking Proteins. Adapted from [28].

Despite the known significance of both processes described in neuronal development and regeneration, here we will focus mainly on MT function and dynamics. Microtubules are the stiffest of the three cytoskeleton polymers and present the most complex assembly and disassembly dynamics [27]. The molecular building block of this structure is the tubulin subunit, a heterodimer of α- and β-tubulin. These subunits bind and form structurally polarized protofilaments, which associate laterally to form a tube with an outer diameter of approximately 25 nanometers [26]. Besides cellular support, MTs are highly important in axonal transport, being the routes along which vesicles, organelles and proteins are transported by kinesin and dynein (Figure 7) [29].

Microtubules are highly dynamic and are able to switch between stably growing and rapidly shrinking states. These phenomenon is known as dynamic instability and was first described in 1984 [30]. As depicted in Figure 6, these structures grow by the addition of GTP-tubulin dimers to the microtubule end, where a stabilizing cap forms. Below the cap, tubulin dimers are in the GDP-bound state. When this stabilizing cap is lost, the MT shrinks rapidly in a process known as catastrophe. These shrinking MTs might be rescued, switching back to the stable growth state [30, 31]. Dynamic instability allows MTs to explore cellular regions and retract in case they do not find a suitable environment [32].

Although both the minus-end, on the soma side, and the plus-end, which faces the axonal tip, of MTs are capable of growth and shrinking, the latter grows faster and has a higher catastrophe rate [33]. The plus-end is also crucial in regulating MT dynamics, since it is where the accumulation of regulatory proteins, such as plus-end tracking proteins (+TIPs), takes place. These proteins are a type of microtubule-associated protein (MAP) and are able to regulate different aspects of neuronal development and function by controlling MT growth and catastrophe events [33].

End-binding (EB) proteins are among the +TIP complex and are known to interact with other +TIPs and recruit many of them to the growing MT ends [33]. Within the several proteins belonging to the EB family, EB3 has been shown to be preferentially expressed in the central nervous system [34]. Fluorescently tagging EB proteins has been widely used

as a way of tracking growing MTs [35, 36] which can be a valuable tool in neuronal regeneration studies.

Besides +TIPs, there are a number of other regulators of MT dynamics, namely the associated motor proteins or the tubulin post-translational modifications, as schematically represented in Figure 7.

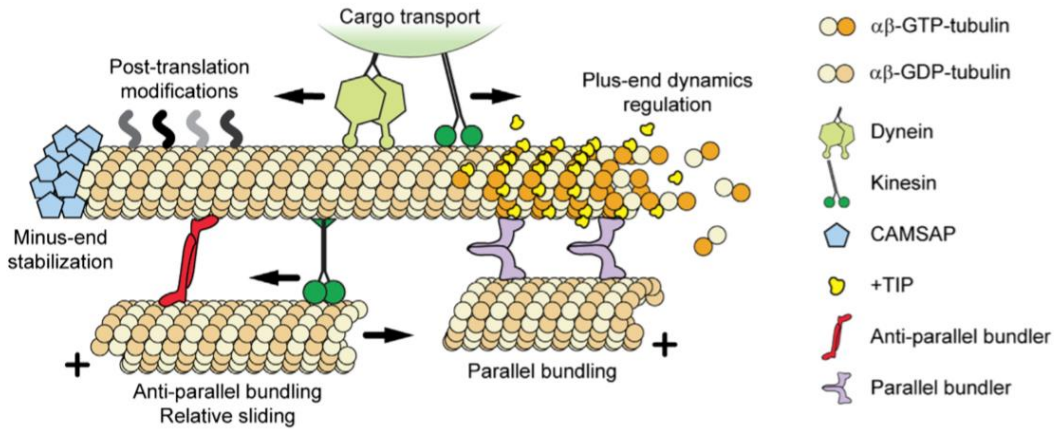

Figure 7 - Microtubule Dynamics Regulators. Cartoon illustrating how different microtubule-related proteins interact with microtubules. Adapted from [31].

Recently, cytoskeleton dynamics has been emerging as an appealing target to promote axon regeneration [37], as it will be further discussed.

Microtubule Dynamics and Axon Regeneration

A major obstacle to CNS regeneration is the inability of adult central neurons to form a growth cone following axotomy [38]. These structures are responsible for axon elongation, since they integrate extracellular signals and are able to guide growing axons to reach their correct targets [39].

Growth cones present a very particular spatial organization and dynamics of the cytoskeleton. As shown in Figure 8, in the center of growth cones, dynamic microtubules protrude from the axonal shaft, while on the periphery, long bundles of actin radiate outward, giving rise to filopodia. These radial actin bundles are tangled by meshes of actin, the lamellipodia. Microtubules in the axon shaft are more stable, while the ones that extend to the center undergo more dynamic events [37].

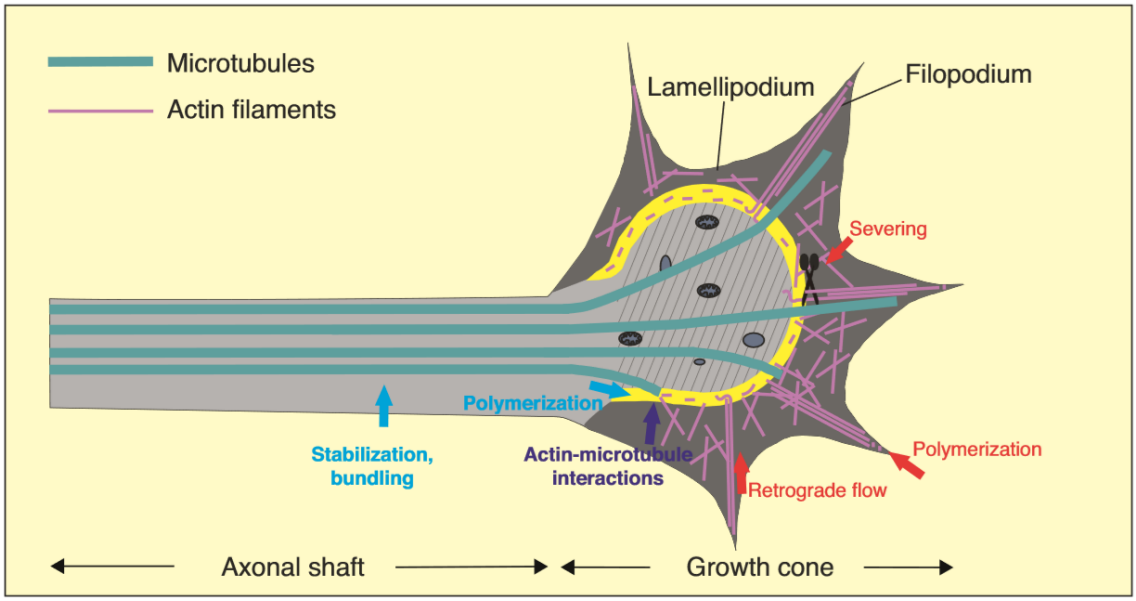

Figure 8 - Cytoskeletal Organization of Elongating Axons. The axonal shaft of elongating axons contains stable microtubules whereas their growth cone contains a dynamic cytoskeleton. In the center of growth cones (grey stripped area), dynamic microtubules protrude from the axonal shaft. More peripherally (dark grey area), long bundles of actin radiate outward, giving rise to the filopodia. Meshes of actin filaments, the lamellipodia, intertwine these radial actin bundles. Red and blue arrows represent the main cytoskeletal dynamics leading to axon elongation, respectively for actin and microtubules. Adapted from [37].

Altogether, the growth cone of developing or regenerating neurons provides an environment in which polymerizing microtubules can protrude and originate axon elongation. Hence, before a cut axon can grow through an inhibitory environment, it first has to be able to assemble a new growth cone at its tip. However, it has become clear that CNS neurons fail at this fundamental step [38].

Instead of a growth cone, injured CNS neurons form a retraction bulb at the tip [39, 40]. These structures, first described by Ramon y Cajal [11], are about four times larger than the injured axon and continue to grow overtime [39] and, unlike in growth cones, cytoskeleton elements majorly overlap in retraction bulbs [40]. Additionally, great part of MTs undergoes depolymerization, while the rest become disorganized and unable to reach the axon tip [39]. A comparative view of growth cones and retraction bulbs is given in Figure 9.

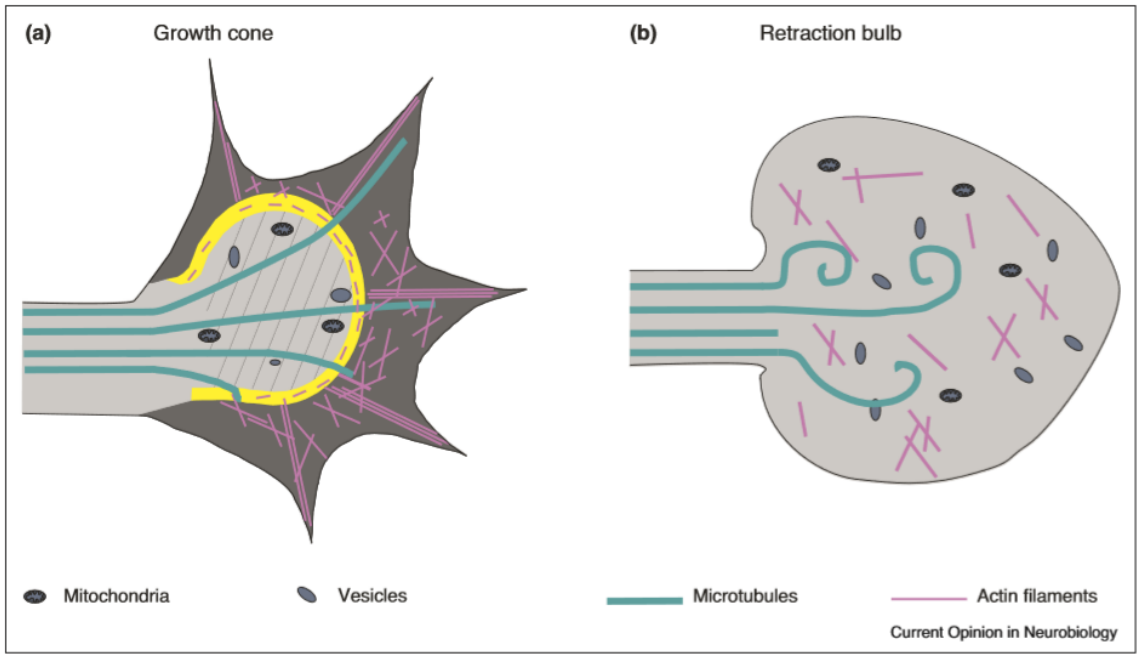

Figure 9 - Cytoskeletal Organization in Growth Cones versus Retraction Bulbs. A| Growth cones display distinct regions. The center (grey stripped area) contains microtubules which emerge from the axonal shaft. In the periphery (dark grey area) a dense network filaments controls the progression of microtubules towards the axon tip. **B|** In retraction bulbs the separation between different domains is lost. In addition, microtubules are depolymerized to a large extent. The remaining ones are disorganized and do not reach the axon tip. Adapted from [37].

The question that needs to be answered in order to develop new therapies that enable CNS axon regeneration is: how do we go from retraction bulbs to growth cones?

Previous work has shown that treating dorsal root ganglia (DRG) neurons with microtubule-depolymerizing drug nocodazole leads to the formation of retraction bulb-like structures [39]. In contrast, administration of epothilone B, an enhancer of MT polymerization, not only reduces the generation of retraction bulbs, but also enhances axon regeneration after SCI [41]. Identically, the stabilizer agent taxol improves growth cone formation in adult injured CNS neurons [42, 43].

Together, these data provide evidence that the inability of adult central neurons to efficiently form a growth cone is related with microtubule dynamics and that controlling this property might be the key to improve their regenerative capacity.

Besides restoring growth cones, targeting the cytoskeleton may further promote regeneration by modifying axonal transport, since this structure is responsible for ensuring intracellular trafficking [29]. When an injury takes place, an "injury signal", triggered by calcium influx [14, 24], is sent to the nucleus. This retrograde signaling (from the axon tip to the soma) is dependent of the transport of several molecules, such as transcription factors, along microtubules [44, 45]. Deficient retrograde transport may give rise to CNS neurons inability to put on a pro-regenerative program. Retraction bulbs are thought to be associated with this deficiency, since they are much larger than the axon and possess a higher density of mitochondria and small vesicles [39]. Anterograde transport of organelles and material to the tip of the axon is also required for and a limiting factor of regenerative processes [46]. The need of a microtubule-binding domain with anterograde transport activity for the pro-regenerative action of some proteins [47] supports this correlation. Interfering with MT dynamics can improve anterograde transport to the growth cone to supply necessary elements and enhance axon re-growth.

Recently, it has also been emphasized the possibility of decreasing the formation of inhibitory surroundings by targeting the cytoskeleton. It has been shown that stabilizing the microtubule network reduces fibroblasts migration towards the lesion site [41] and prevents the release of inhibitory proteins by astrocytes and fibroblasts [41, 42, 48].

In summary, modifying cytoskeleton-dynamics is a multifaceted strategy which can restore growth cones, enhance axon growth and reduce the environmental inhibition to axon regeneration. Hence, this dynamics represents an appealing target and may hold promise as a basis for the development of a regenerative therapy after a spinal cord injury.

Modifying Microtubule Dynamics

Although molecular players leading to pro-regenerative cytoskeletal rearrangements are still not fully understood, several modulators of MT dynamics are known and used as therapeutic targets. Within the scope of this thesis, the highlight will be the post-translational modifications (PTM) that occur on MT.

These modifications have been increasingly recognized as crucial controllers of MT properties and functions [49]. A wide range of PTMs is known to occur on tubulin (Figure 10|A). Among the better-studied are detyrosination, Δ2-tubulin generation, polyglutamylation, polyglycylation and acetylation [50].

Here, we will focus on the acetylation of the lysine 40 (Lys40) residue of α-tubulin, which was the second tubulin PTM to be discovered [51]. This modification takes place on the lumen of MTs [52], as depicted in Figure 10|C. Only many years after the discovery of this modification was possible to identify the deacetylating enzymes: histone deacetylase 6 (HDAC6) [53] and sirtuin-2 (SIRT2) [54]. Although both these enzymes are homologues of histone deacetylases, their activity occurs mostly towards α-tubulin and other cytoplasmic constituents, rather than histones, since they primarily function in the cytoplasm and not in the nucleus [53, 54].

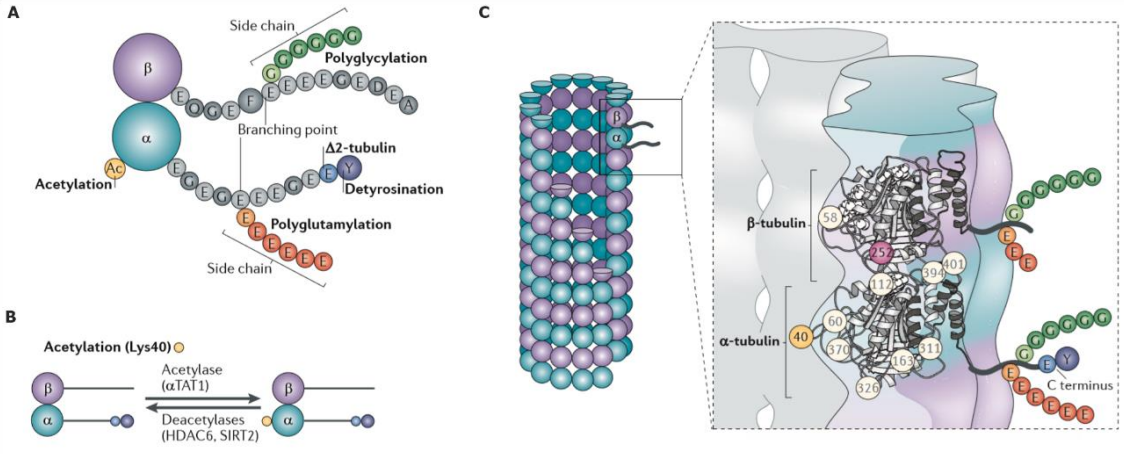

Figure 10 - Tubulin Post-Translational Modifications. A| Schematic representation of the α-tubulin-β-tubulin dimer and its associated modifications. **B|** Schematic representation of the generation and removal of α-tubulin acetylation. **C|** Localization of tubulin PTMs. Acetylation of α-tubulin Lys40 is exposed to the luminal face of microtubules. All modifications are shown using the color code detailed in part A. Abbreviations: αTAT1 - α-tubulin N-acetyltransferase 1; HDAC6 - Histone Deacetylase 6; SIRT2 - Sirtuin 2; PTM – Post-Translational Modifications; Lys40 - Lysine Residue 40. Adapted from [50].

Acetylated tubulin is enriched in older, stable microtubules along the axon shaft and, therefore, it is the PTM more frequently correlated with MT stability [50]. It has been shown that acetylated microtubules are more stable, to the extent that are able to withstand mild treatment with MT-depolymerizing drugs [55, 56]. Conversely, decreased levels of acetylated α-tubulin and consequent impairments in axonal transport have been reported in several neurodegenerative diseases, namely Alzheimer's [57], Parkinson's [58], Huntington's [59] and Charcot-Marie-Tooth [60].

Since moderate microtubule stability has already been reported as required to promote axon growth and regeneration [39, 42], drugs that target MT-acetylation appear as a useful strategy to enhance axon re-growth after injury. Nevertheless, the impact of modulating acetylating or deacetylating enzymes on MT stability is not fully clear, since determining the roles of the different modifications *in vivo* is challenging because PTMs rarely occur in isolation and the level of each modification is singularly regulated by the cell [50].

ACY-738 (N-hydroxy-2-(1-phenylcycloproylamino)-pyrimidine-5-carboxamide) is a novel small molecule inhibitor of HDAC6, developed by Acetylon Pharmaceuticals. HDAC6 constitutes a good target firstly because it is located in the cytoplasm [53], hence not affecting DNA expression, and additionally because it presents two catalytic domains [61] and therefore an increased deacetylase activity. Studies show that inhibition of this deacetylase reduced the velocities of MT growth and shrinkage [62], enhanced the capacity of DRG neurons to grow on inhibitory substrates and could promote survival and regeneration of injured neurons [63].

ACY-738 demonstrates inhibitory activity against recombinant HDAC6 with half minimal inhibitory concentration (IC_{50}) values of 1.7 nM and with average selectivity over other HDACs being 100-fold [64]. Compared with other inhibitors, ACY-738 presents an improved bioavailability, as it is able to efficiently cross the blood-brain-barrier [64].

Several studies have reported the beneficial effects of this drug in several conditions, such as Alzheimer's disease [65], systemic lupus erythematosus [66] and vincristine-induced neuropathies [67].

Altogether, these data establish ACY-738 as a cytoskeleton-targeting drug that could be explored as a potential therapy for spinal cord injuries.

This drug is being tested in two parallel projects, using either a model of spinal cord injury or a model of neurodegeneration.

COMBINE Project

The COMBINE Project results from a cooperation between IBMC.INEB researchers, Centro de Reabilitação do Norte and Acetylon Pharmaceuticals. It aims at developing a combinatorial regenerative strategy to potentiate axon regeneration and improve functional recovery after spinal cord injury.

The novel therapeutic strategy targets both the cell-intrinsic properties of CNS neurons and the extrinsic inhibitory environment of the injured spinal cord. This pro-regenerative approach would eventually be combined with a specific rehabilitation program.

Currently, in the context of this project, the Nerve Regeneration Group is performing the *in vivo* evaluation of ACY-738, using a clinically relevant model: a spinal cord contusion injury in rats, since, unlike mice, these animals form cysts at the impact site [68] as seen in human patients [4].

Even though the use of ACY-738 as part of a combinatorial therapy for spinal cord is the final goal, the work developed in this thesis focused rather on the *in vitro* outcomes in the presence of the drug than on the *in vivo* evaluation as part of the COMBINE project.

The Twitcher Mouse

Assessing neurite outgrowth and microtubule dynamics *in vitro* is necessary in order to adequately characterize the effects of the drug and understand its mechanisms of action. To study these processes, experiments were conducted using both twitcher mice neurons, as a model for degeneration, and wild type (WT) neurons to compare the action of the drug in distinct scenarios.

The twitcher mouse is a model for globoid cell leukodystrophy, most known as Krabbe's disease [69]. This disease is a lysosomal storage disorder caused by an impairment in the activity of beta-galactosylceramidase

(GALC) [70, 71]. Deficient GALC activity leads to an accumulation of its substrates, namely galactosylceramide and psychosine [72, 73]. Galactosylceramide (Gal-Cer) is the principal glycosphingolipid in the brain tissue. During myelin turnover, GALC breaks Gal-Cer down into galactose and ceramide, and these products are re-used in a separate remyelination pathway [72, 73]. In Krabbe's disease, this does not occur and there is an accumulation of free Gal-Cer, which as a specific capacity of triggering infiltration of macrophages into the brain. Once in the brain, they phagocytize Gal-Cer and originate multinucleated globoid cells [74]. Hence, the loss of GALC enzymatic activity leads to myelin degeneration since remyelination does not occur effectively but myelin turnover continues [72, 73]. Additionally, there is also an accumulation of psychosine, which is known to be cytotoxic for myelin-forming cells [72, 73].

The twitcher mouse is a neurological mutant which closely mimics the most common form of the human disease and was first discovered in 1976 in the mouse colony of the Jackson Laboratory [75]. The fundamental genetic defect in this model is a premature stop codon in the galc gene which abolishes GALC enzymatic activity. This mutation is inherited in a Mendelian autosomal recessive way [76]. Since cDNA for murine GALC has already been cloned [77], successful approaches using gene therapy to rescue the twitcher mouse phenotype have already been reported [78].

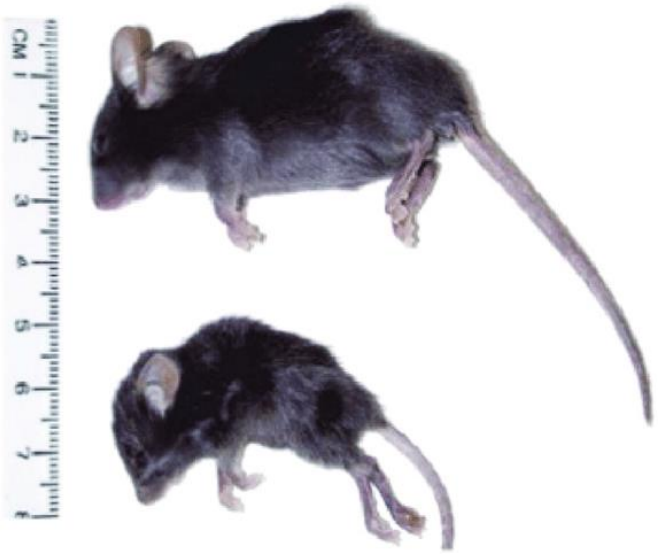

Figure 11 - Wild-type versus twitcher mouse. Lose weight and a hunched back are characteristic of the twitcher mouse. 42-day old littermates: Upper mouse, wild-type; lower mouse, twitcher. Adapted from [78].

Although no obvious clinical signs are present at birth or during early stages of development, around 20-22 days after birth, homozygous affected mice start showing neurologic signs such as tremulousness, particularly of the head, incoordination of the limbs and hind limb paralysis. As the disease progresses, weight loss and more prominent muscular weakness (particularly in the hind limbs) are also registered and the size difference becomes pronounced (Figure 11). Heterozygous carrier mice are entirely normal phenotypically. In advanced stages of the disease, there is a severe degeneration of myelin throughout the central nervous system and axonal degeneration also occurs. Hence, twitcher mice usually don't survive past post-natal day 45 [69].

It has been previously been described that twitcher neurons have lower levels of acetylated tubulin [79] and, therefore, our group has established a partnership with Acetylon Pharmaceuticals to assess the effect of ACY-738 in this model.

II. MATERIALS AND METHODS

1. Animals

Twitcher (twi) mice and wild-type (WT) littermates were obtained from heterozygous breeding pairs (Jackson Laboratory) and were bred in the animal house facility of i3S with *ad libitum* access to water and rodent food, and were kept on a 12 hour light and dark cycle. All mice were handled and euthanized according to the i3S humane endpoints standard operation procedure established according to FELASA's recommendations (www.felasa.eu) when any of the following features was observed: severely impaired mobility, prolonged dehydration, decreased food intake (for more than 72 hours) or severe weight loss (more than 20%).

2. Genotyping

Genotyping of twitcher mice is based on the use of deoxyribonucleic acid (DNA) extracted from the mice and a mismatched primer that creates a restriction site for EcoRV if the allele possesses the mutation [77]. At PND 10, ear fragments were collected from mice and DNA was isolated and amplified by the Cell Culture and Genotyping group (CCGen).

For purification, sodium acetate (NaOAc; Sigma-Aldrich, S8750) was mixed with DNA, to allow the precipitation of proteins. Adding sodium iodide (NaI; Enzymatic, S/5130/53) lead to the binding of DNA to silica (Si^+) (Silicon Dioxide; Sigma-Aldrich, S5631) particles; this DNA was then washed twice and eluted in tris-ethylenediaminetetraacetic acid (EDTA) (TE) buffer (Invitrogen, 8019005).

After purification, the samples were mixed with an enzyme-containing solution (Eco32I; Thermo Fisher Scientific, ER0301) and maintained overnight (ON) at 37°C.

Digestion products were run in a 4% agarose (Agarose LM Ultrapure Grade; NZYTech, MB12301) gel electrophoresis for 50 minutes at 130 volts (V) and 300 milli-amperes (mA). The gel contained GreenSafe Premium (NZYTech, MB13201) and was revealed in a Gel-Doc-XR system (BioRad).

The resulting digestion pattern can be interpreted to define the genotype of each animal. An upper band of 260 base pairs (bp) is from a non-mutated allele and a lower band of 234 bp is from a mutated allele. Therefore, one upper band defines the mouse as a wild-type and one lower band defines it as an affected twitcher mouse. If two bands are present, then the mouse is heterozygous (het) [77].

3. Primary Culture of Dorsal Root Ganglia (DRG) Neurons

DRG were isolated from twitcher mice and WT littermates. The nodules were collected to Dulbecco's Modified Eagle Medium: Nutrient F12 ham (DMEM:F12; Sigma-Aldrich, D8437) supplemented with 10% fetal bovine serum (FBS; Sigma-Aldrich, F9665) and 1% penicillin/streptomycin (P/S; Invitrogen, 15140-122).

DRG were digested with collagenase IV-S (Sigma-Aldrich, C1889) for 1 hour and 30 minutes, mixing every 30 minutes, and washed 3 times with DMEM:F12. Modified glass Pasteur pipettes of decreasing diameter were used to obtain a suspension with no visible clumps of cells. Neurons were isolated centrifuging the cell suspension into a 15% bovine serum albumin (BSA; Sigma-Aldrich, A3294) cushion, for 10 minutes at 1000 rpm. Interphase and supernatant were discarded and cells were ressuspended on DMEM:F12 supplemented with 1% P/S, 2× B27 (Invitrogen, 0080085SA), 2 mM L-glutamine (L-Glu; Invitrogen, 25030024) and 50 ng/mL nerve growth factor (NGF; Merck Millipore, 01-125). Cells were further used for Neurite Outgrowth or Microtubule Dynamics assays, as described below.

4. Neurite Outgrowth Assay

The cells were plated in the presence of dimethyl sulfoxide (DMSO; Sigma-Aldrich, D5879) 0.1% or ACY-738 (Acetylon Pharmaceuticals) 100 nM in DMSO, at a density of 7500 cells per well in coverslips coated with 20 µg/mL poly-L-lysine (PLL) in phosphate buffer saline (PBS) (incubated for 1 hour at 37ºC) and 5 µg/mL laminin in PBS (incubated for 30 minutes at 37ºC). After plating, the cells were maintained at 37ºC in a 5% carbon dioxide (CO_2) atmosphere.

At day *in vitro* (DIV) 3 half of the culture medium was removed and complete media was added, maintaining a final concentration of 0.1% DMSO or 100 nM ACY-738 in culture. Cells were fixed in 4% paraformaldehyde (PFA; Sigma-Aldrich, 158127) in PBS either at DIV1 or DIV5.

4.1. βIII Tubulin Immunocytochemistry

Fixed cells were permeabilized with 0.2% Triton X-100 (Sigma-Aldrich, T9284) in PBS, blocked for 1 hour at RT in 5% FBS in PBS and incubated ON at 4°C in Guinea Pig anti-βIII-tubulin (Synaptic Systems, 302 304) at 1:1000 in blocking buffer.

After incubation with Alexa Fluor 488-conjugated AffiniPure Donkey Anti-Guinea Pig (Jackson ImmunoResearch Laboratories, 706-545-148) 1:1000 in blocking buffer, for 1 hour at RT, coverslips were mounted in Fluoroshield with DAPI (Sigma-Aldrich, F6057), sealed and stored in the dark at 4°C.

Immunostained neurons were visualized with a Motorized inverted epifluorescence microscope, LEICA DMI 6000 FFW, using the 10x objective.

4.2. Neurite Outgrowth Quantification

Tiff 8-bit images were opened with the Synapse Detector (SynD) program, developed for the automated analysis of neuronal morphology [80]. The program automatically detects the soma and traces neurites (using steerable filters), but all the results were manually corrected. Only neurons with neurites larger than the diameter of the cell body were considered.

The parameters used for the evaluation of neurite outgrowth were the Total Neurite Length and the neurite branching, described by a Sholl Analysis.

5. Microtubule Dynamics Assay

5.1. EB3 Transfection

After centrifuging for 5 minutes at 800 rpm, the supernatant was discarded and cells were ressuspended in 20 µL of Opti-MEM® I Reduced Serum Medium (Invitrogen, 31985047) containing 250 ng of pEGFP-EB3. The cells were transferred to a Nucleocuvette™ Strip and transfected using the PM-137 program (Mouse DRG Neurons) of the 4D-Nucleofector™ (Lonza). After 10 minutes of resting at 37°C, 80 µL of RPMI 1640 Medium, GlutaMAX™, HEPES (Invitrogen, 72400-021) supplemented with 10% FBS was added. Cells were added to complete media (without drug or DMSO) and let in suspension for 24h at 37°C in a 5% CO_2 atmosphere.

At DIV1, cells were plated at a density of 10 000 cells/well in glass-bottom 8-well µ-dishes, coated with 20 µg/mL PLL in PBS (incubated for 1 hour at 37°C) and 5 µg/mL laminin in PBS (incubated for 30 minutes at 37°C). At DIV4, the medium was changed to complete media without phenol red and at DIV5, two hours before imaging, half of the medium was replaced with complete media without phenol red supplemented with DMSO or ACY-738. Final concentrations in culture were 0.1% DMSO or 100 nM ACY-738.

Transfected cells were visualized using the 100x objective of the spinning disk confocal system Andor Revolution XD, with controlled temperature and CO_2 conditions. Time-lapse recordings (a total of 60 frames, every 2 seconds) were acquired in three planes separated by 0.2 µm each.

5.2. Microtubule Growth Speed Quantification

Using the ImageJ software, resulting files were converted to a hyperstack (1 channel, 3 slices, 60 frames) and a z projection was applied for each frame (Start slice: 1, Stop slice: 3, Projection Type:

Max Intensity), in order to obtain a single stack that could be further analyzed.

Stacks were analyzed using the KymoResliceWide plugin to build kymographs of the region of interest. Kymographs are a way to represent a dynamic process in a single image, where we move along space in the x direction and along time in the y direction. Kymographs were built using maximum intensity across the line and several lookup tables were tested in order to better visualize the existing comets, as shown in Figure 12. Initial and final positions in x and y axis were marked and measured using the Cell Counter plugin, in order to calculate the growth speed (length in the x direction (distance) over length in the y direction (time)). Only comets with three or more steps were considered.

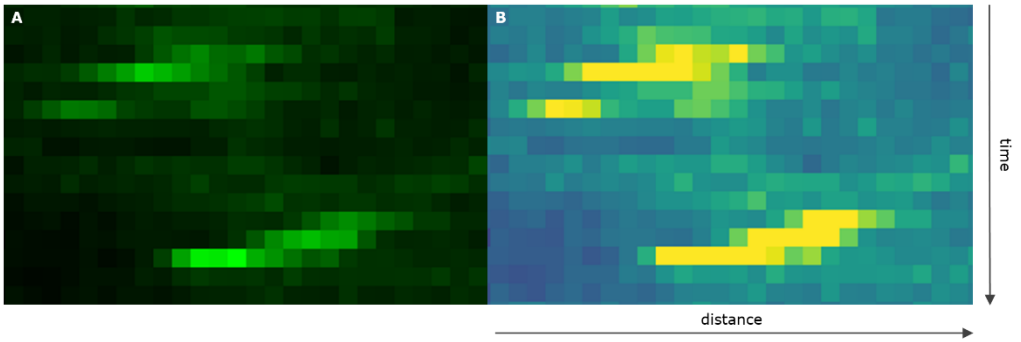

Figure 12 - Kymographs for Microtubule Growth Speed Quantification. Kymographs obtained with ImageJ plugin KymoResliceWide. The original kymograph (**A|**) was modified by changing the lookup table, obtaining a better visualization of the existing comets in the modified kymograph (**B|**). Only comets with three or more steps were considered: upper comet was excluded, lower comet was included.

III. Results and Discussion

Genotyping

Genotyping allows the detection of small genetic differences that can lead to major changes in phenotype, namely pathological changes underlying disease. This process is essential in order to correctly establish the experimental conditions used in our studies. As described in the Materials and Methods Section, the genotyping of twitcher mice is based on the use of a mismatched primer that creates a restriction site for EcoRV if the allele possesses the mutation [77]. The different digestion patterns allow the distinction between heterozygous, WT and twitcher mice, as described in Figure 13.

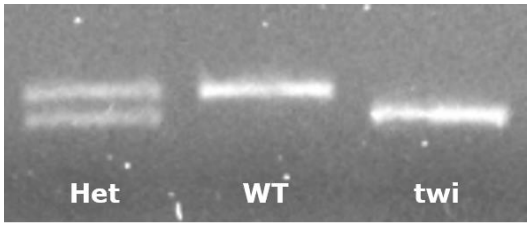

Figure 13 - Digestion Patterns of genomic PCR fragments. Following restriction digestion, an upper band defines a non-mutated allele and a lower band defines a mutated allele. Therefore, a single upper band defines the mouse as a WT and one lower band defines it as an affected twitcher mouse. If two bands are present, then the mouse is heterozygous. Abbreviations: Het – Heterozygous; WT – Wild Type; twi – twitcher.

ACY-738 inhibits neurite outgrowth *in vitro*

Assessment of neurite outgrowth *in vitro* is an easy way to determine the effects of an exogenous factor, in this case ACY-738, on neurons behavior. WT and twitcher mice DRG neurons were treated with the drug or, to use as a control, with DMSO, the vehicle. Results are presented as the mean ± standard error of the mean (SEM) of the results of a minimum of 111 individual cells per condition.

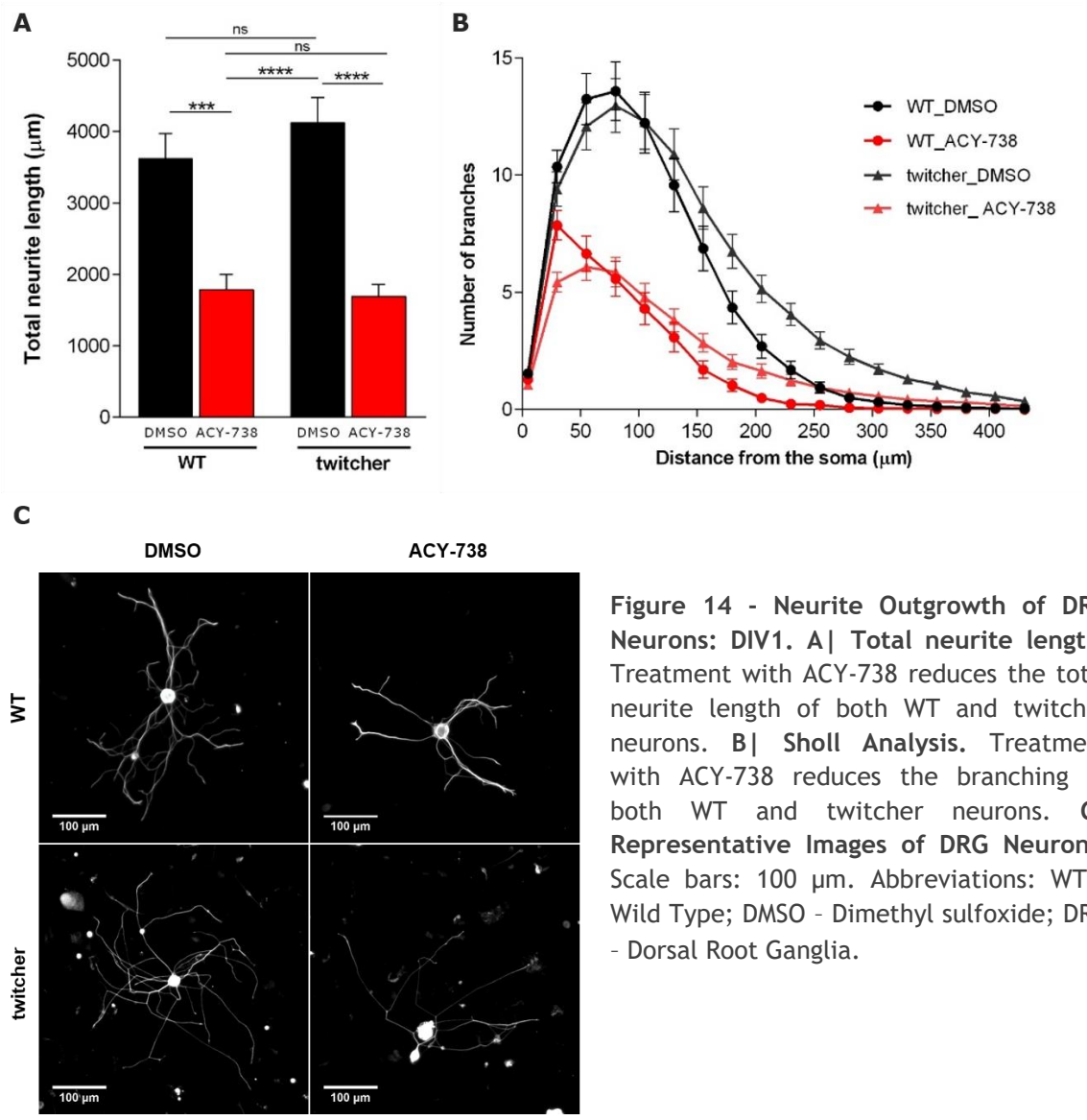

Figure 14 - Neurite Outgrowth of DRG Neurons: DIV1. A| Total neurite length. Treatment with ACY-738 reduces the total neurite length of both WT and twitcher neurons. **B| Sholl Analysis.** Treatment with ACY-738 reduces the branching of both WT and twitcher neurons. **C| Representative Images of DRG Neurons.** Scale bars: 100 μm. Abbreviations: WT – Wild Type; DMSO – Dimethyl sulfoxide; DRG – Dorsal Root Ganglia.

At DIV1, WT neurons treated with only DMSO presented an average total neurite length of 3620±3938 μm (n=125), while neurons treated with ACY-738 had an average length of 1786±2267 μm (n=111). This represents a 2 fold decrease ($p \leq 0.001$; Figure 14|A) in the total neurite length of DRG neurons following treatment with ACY-738. Similarly, in twitcher neurons treatment with ACY-738 resulted in a decreased total neurite length of 1692±1888 μm (n=124) when compared with only DMSO, where the average length was 4125±4178 μm (n=144). These results correspond to a 2.4 fold decrease ($p \leq 0.0001$; Figure 14|A) after treatment with the drug. Besides lower neurite lengths, presence of ACY-738 in culture also resulted in decreased branching of both WT and twitcher neurons (Figure 14|B).

Regarding WT and twitcher neurons subjected to the same treatment (either DMSO or ACY-738), there were no differences. Representative images of neurons of each condition are presented in Figure 14|C.

Since ACY-738 is already known to enhance the capacity of DRG neurons to grow on inhibitory substrates and to promote survival and regeneration of injured neurons [63] this consistent decrease in neurite outgrowth *in vitro* following treatment with the drug was not expected. However, studies reporting these results focused on neurite growth under inhibitory conditions and did not evaluate the effect that HDAC6 inhibition had on basal neurite outgrowth.

Recently, α-tubulin acetyltransferase (α -TAT1) has been reported as a target mediating the neurite growth inhibitory effects of CSPGs [81]. In the presence of these molecules, a RhoA-kinase-dependent decrease in α-tubulin acetylation and in α-TAT1 protein levels was described, without any changes to HDAC6 levels or activity. Inhibition of the RhoA-kinase or α-TAT1 overexpression restored neurite growth [81]. Since HDAC6 is the opposing enzyme to α-TAT1, this data suggests that the inhibition of HDAC6 activity would also promote DRG neurons outgrowth in inhibitory conditions [63] by reversing the effect of extrinsic molecular barriers to axon growth and not by intrinsic mechanisms of cytoskeleton modulation.

However, it is not clear why treatment with ACY-738 results in such a marked decrease of the total neurite length and the branching of DRG neurons. Since this is a very early time point, the stabilization of microtubules may have prevented the formation of a functional growth cone, given that a strong dynamics is needed to establish these structures. The lack of a well-structured growth cone would explain the inhibition that was observed in the neurite outgrowth assay.

At DIV5, ACY-738 has a neuroprotective effect on twitcher DRG neurons

At DIV5, treatment with ACY-738 had a similar effect on WT neurons as the one observed at DIV1. WT DRG neurons treated with DMSO have an average total neurite length of 2006±1899 μm (n=117) and treatment with ACY-738 results in a 1.7 fold decrease ($p \leq 0.0001$; Figure 15|A), with an average length of 1192±750 μm (n=92). Conversely, treatment of twitcher neurons with ACY-738 showed a tendency to increase the total neurite length by 1.3 fold, from 964±662 μm (DMSO; n=73) to 1335±1127 μm (ACY-738; n=67). However, this tendency was not statistically significant ($p > 0.05$; Figure 15|A).

Regarding WT and twitcher neurons treated with only DMSO, at DIV5 there was a 2.1 fold decrease ($p \leq 0.0001$, Figure 15|A) of total neurite length in twitcher neurons. Treatment with ACY-738, on its side, resulted in an absence of significant differences between WT and twitcher neurons.

The decreased length observed in twitcher DRG neurons compared to WT neurons, when treated with only DMSO, is concordant with previous studies [79]. It was reported that, from DIV5 on, twitcher DRG neurons in culture started evidencing axonal swellings and there was a decrease in the percentage of cells which presented neurites. This neurite degeneration in twitcher neurons was suggested to be the reason of neurite outgrowth failure overtime, despite the initial growth-competent state [79]. Our data suggests that ACY-738 is able to rescue, at least partially, this effect, since there are no significant differences between WT and twitcher neurons treated with the drug. The fact that ACY-738 has a beneficial effect in this degenerative context is in agreement with previous reports of its effects in several neurodegenerative disorders [65-67].

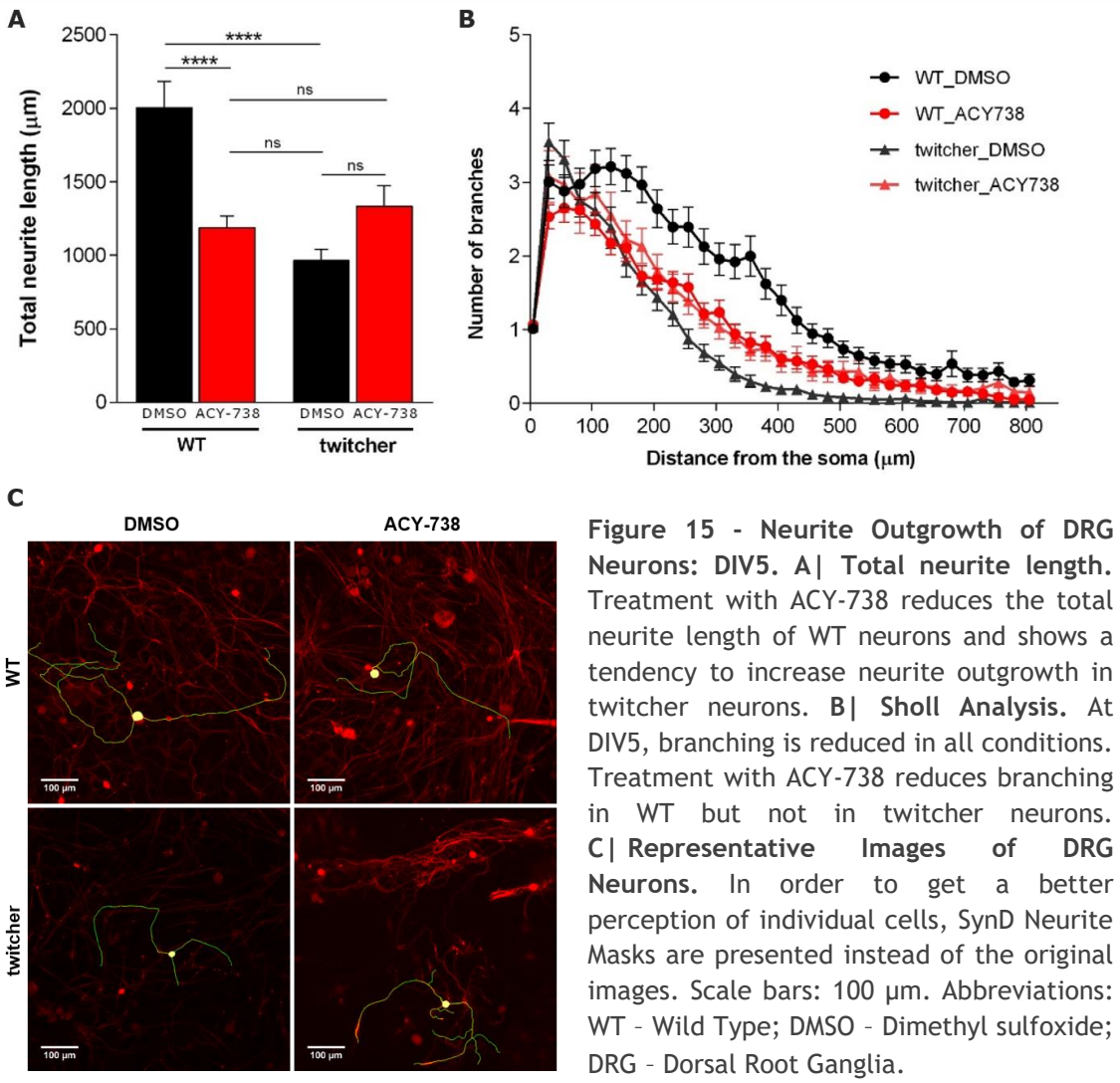

Figure 15 - Neurite Outgrowth of DRG Neurons: DIV5. A| Total neurite length. Treatment with ACY-738 reduces the total neurite length of WT neurons and shows a tendency to increase neurite outgrowth in twitcher neurons. **B| Sholl Analysis.** At DIV5, branching is reduced in all conditions. Treatment with ACY-738 reduces branching in WT but not in twitcher neurons. **C| Representative Images of DRG Neurons.** In order to get a better perception of individual cells, SynD Neurite Masks are presented instead of the original images. Scale bars: 100 µm. Abbreviations: WT – Wild Type; DMSO – Dimethyl sulfoxide; DRG – Dorsal Root Ganglia.

Regarding the effect that ACY-738 had on WT neurons at DIV5, although it was unexpected, it is very consistent with the observations at DIV1. The reason for this inhibition is still not understood. Previous work by our group had already used the same concentrations of both DMSO and ACY-738 in culture for axonal transport experiments. In these conditions, cultures in the presence of ACY-738 increased the axonal transport of mitochondria (unpublished data), suggesting that the concentrations of DMSO or ACY-738 are not the reason for these unexpected results.

ACY-7738 is reported to have a half-life of 12 minutes in plasma [64]. Considering this, a factor which may be influencing the action of the drug is its time of action in culture. If the short half-life in plasma is translated to a

short time of action in culture, the unexpected inhibition of neurite outgrowth can be due to a not proper design of the experience. Following the culture, medium is only supplemented with more ACY-738 or DMSO at DIV3. Additionally, cells are only fixed one or two days after the last supplement. This results in large time gaps in which the drug is probably not having any effect. The switching between the drug's action and its absence may be influencing the ability of neurons to grow and be the cause of the reported inhibition of neurite outgrowth in DRG neurons treated with ACY-738. Supplementing the medium with ACY-738 or DMSO more frequently, or adding them a few hours before fixation may lead to different outcomes. Nevertheless, the neurite outgrowth assay must be repeated in the same conditions in order to validate these results and exclude the possibility that they are due to any problem during the culture.

In the future it might be of interest to add another time point to this assay. Assessing neurite outgrowth later than DIV5 will allow us to follow the possible progression of the neuroprotective effect of ACY-738 on twitcher neurons, additionally to validating the results previously shown.

Twitcher growth cones dynamic behavior is rescued following treatment with ACY-738

Tubulin acetylation is generally seen as a modification that characterizes stable microtubules. Using EB3-GFP as a marker of microtubule growth in live cells, we analyzed microtubule dynamics in WT and twitcher neurons, treated with ACY-738 or with DMSO alone. For each cell, microtubule growth speed was quantified separately in the axon shaft and in the growth cone. Results are presented as mean ± SEM of individual comets growth speed.

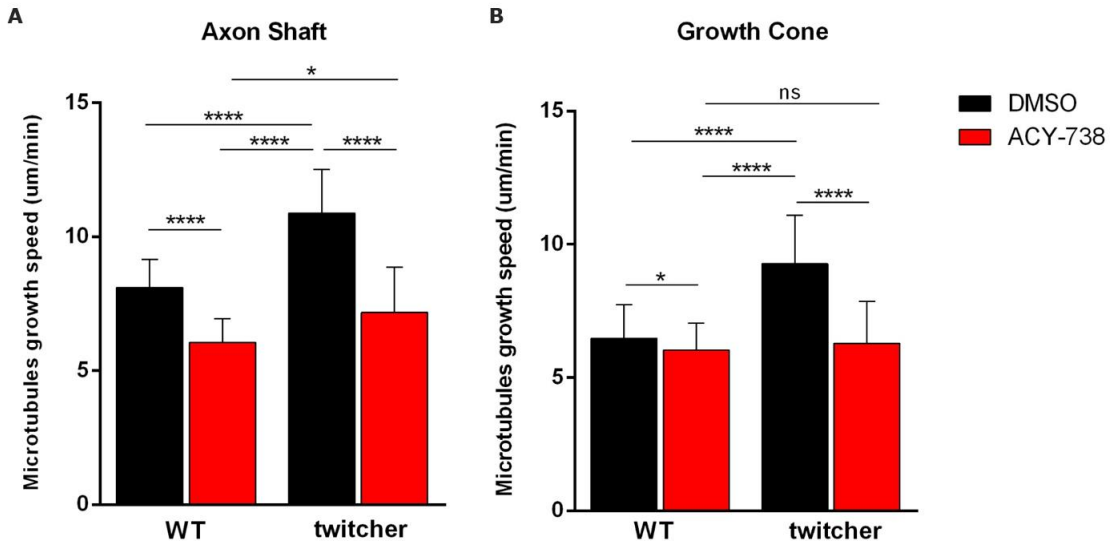

Figure 16 - Microtubule Growth Speed. A| Axon Shaft. In the axon shaft, treatment with ACY-738 reduces the microtubule growth speed of both WT and twitcher DRG neurons. **B| Growth Cone.** In growth cones, ACY-738 causes a decrease of both WT and twitcher neurons microtubule growth speed. Abbreviations: WT – Wild-Type; DMSO – Dimethyl Sulfoxide.

Concerning the axon shaft, in both WT and twitcher DRG neurons, treatment with ACY-738 reduced the microtubule growth speed. In WT neurons, there was a 1.3 fold decrease, from 8.1±1.0 μm/min (n=31) to 6.1±0.9 μm/min (n=22; $p \leq 0.0001$; Figure 16|A); in twitcher neurons, treatment with ACY-738 reduced the growth speed from 10.9±1.6 μm/min (n=49) to 7.3±1.7 μm/min (n=25), which translates into a 1.5 fold decrease ($p \leq 0.0001$; Figure 16|A).

Assessment of microtubule dynamics in the growth cone showed similar results. In WT neurons, there was a slight decrease from 6.5±1.2 μm/min (n=31) to 5.7±1.2 μm/min (n=27; $p<0.05$; Figure 16|B)). In twitcher neurons, the ACY-738 treatment also induced a 1.5 fold decrease of the microtubules growth speed, from 9.3±1.8 μm/min (n=36) to 6.3±1.5 μm/min (n=23; $p \leq 0.0001$; Figure 16|B).

Comparing neurons subjected to the same treatment, the axon shaft of twitcher neurons has an increased growth speed than the axon shaft of WT neurons ($p \leq 0.0001$ for DMSO-only, $p<0.05$ for ACY-738; Figure 16|A). Regarding the growth cone dynamics, while in neurons cultured with only DMSO microtubule growth speed in twitcher growth cones is 1.4 times

higher than WT ($p \leq 0.0001$; Figure 16|B), ACY-738 treatment results in non-significant differences between WT and twitcher neurons, approaching the twitcher microtubules growth speed to that of WT microtubules.

It has been previously shown that twitcher neurons have lower levels of acetylated tubulin and have a higher microtubule growth speed [79], which is consistent with our findings.

In every condition, treatment with ACY-738 resulted in a slower growth speed of microtubules, suggesting that the axons become more stable. Since ACY-738 inhibits HDAC6 and increases acetylation levels, stabilization of the axons was an expected outcome.

Comparing the behavior of WT and twitcher neurons with or without being subjected to treatment with the drug, it is possible to understand that the decrease of microtubule growth speed induced by the drug normalizes the growth speed of twitcher growth cones to WT levels. Although in the axon shaft there are still statistical differences between WT and twitcher neurons treated with ACY-738, the effect of the drug also has the tendency to decrease twitcher microtubule growth speed making it more similar to WT values, probably by increasing their normally low tubulin acetylation levels [79]. This similar behavior of twitcher and WT neurons following treatment with the drug is concordant with the results of neurite outgrowth at DIV5 (Figure 15).

During neurite extension, stable microtubules are needed in the axon shaft to drive forward growth, but those in the growth cone must be highly dynamic to support growth and respond to extracellular stimuli [38]. Comparing the microtubule growth speed in the axon shaft and growth cone of cells treated with DMSO, there are significant differences between the two different regions. However, the same comparison in cells treated with ACY-738 shows no difference between the axon shaft and the growth cone microtubule growth velocities. This suggests that ACY-738 leads to a different, more homogeneous distribution of velocities than the one normally existing in neurons. Although the molecular mechanisms underlying this effect are not clear, this can be the cause for the inhibition of neurite outgrowth evidenced by the presence of the drug, since there is

not a marked difference between a stable axon shaft and a dynamic growth cone.

Although it does not invalidate these results, we must not forget that velocity *per se* is not a measurement of dynamics. In order to get a clear perspective of microtubule dynamics there is a need to quantify the comet density in each region of interest. Combining microtubule growth speed with comet density data it will possible to better interpret the effect ACY-738 has on microtubule dynamics. Other parameters that can be assessed in the future are the catastrophe and rescue rates.

Additionally, it might also be of interest to do a time-frame evaluation of the action of ACY-738. As previously described, the drug might have a short time of action in culture. Therefore, we started imaging 2 hours after supplementing the medium with ACY-738 or DMSO and prioritized conditions in presence of the drug, in order to minimize the effect of time in the results. However, an evaluation of the same condition at different time points may be interesting to elucidate how ACY-738 action in microtubule dynamics changes overtime.

IV. CONCLUSIONS AND FUTURE PERSPECTIVES

Central neurons are unable to mount a pro-regenerative program following injury. Among the several processes which originate this inability, pathological cytoskeleton dynamics have emerged as a major obstacle. Hence, the use of cytoskeleton-targeting drugs may be an efficient strategy to promote regeneration.

Here we intended to evaluate the *in vitro* effects of a microtubule-stabilizer drug and its potential to be used as part of a therapy for SCI. We have shown that ACY-738 inhibits neurite outgrowth *in vitro* for short times in culture but at DIV5 has a neuroprotective effect on twitcher DRG neurons outgrowth. Additionally, twitcher abnormal growth cones dynamic behavior is rescued following treatment with the drug.

Further studies are needed in order to better understand the molecular basis of the results we reported. An assessment of neurite outgrowth after longer times in culture may elucidate how the neuroprotective effect of ACY-738 progresses overtime. Furthermore, measurements of microtubule dynamics combined with studies of the cytoskeletal post-translational modifications occurring along the axon can be of interest to better understand how the drug exerts its effect in the dynamics of the cytoskeleton, which is crucial in order to eventually translate these findings into efficient clinical treatments.

Finally, since our final goal is to use ACY-738 as part of a combinatorial therapy for spinal cord injury (COMBINE Project) it is essential to complement our work with similar *in vitro* studies under inhibitory conditions, similar to the ones existing in an injury scenario.

Chapter 4

Acomys: A Model to Unravel Regenerative Mechanisms in Mammals

I. THEORETICAL BACKGROUND

In mammals, CNS neurons are generally unable to regenerate. Mammals generally do not regenerate as they respond to wounding with scarring, the main cause of their limited regenerative capacity. Nevertheless, the ability of reactivating developmental pathways in later life to restore functional tissues and organs is present in several eukaryotic organisms [82, 83]. Regeneration is found both in invertebrates, as hydra or starfish, and in vertebrates, as fish [84], salamander [85] and axolotl [86]. These species are able to re-grow missing body parts as limbs or the tail, unlike mammals, in which adult regeneration is generally non-existent. However, *Acomys* have recently been described as a potential regenerator mammal.

The African Spiny Mouse: the Regenerator Mammal

Rodents of the genus *Acomys* are collectively referred to as 'spiny mice' due to the bristly fur that emerges from their dorsal skin. They have been classified as a member of the *Muridae* family, a subfamily of rodents that also includes *Mus musculus* and *Rattus novergicus* [87]. However, DNA-DNA hybridization molecular evidence indicates that spiny mice are

more closely related to gerbils (*Gerbillinae* subfamily) than to the true mice and rats (*Murinae* subfamily) [88]. Until now, 18 *Acomys* species have been recognized by the International Union for the Conservation of Nature [89].

The first observations regarding *Acomys* regeneration were reported in 2012 [90]. While handling two different species in the field, tearing of the skin occurred very easily. *Acomys* exhibit skin autotomy as a predator escape behavior, but, unexpectedly, skin regeneration with wound closing and spiny hairs regrowth was found within 30 days (Figure 17) [90].

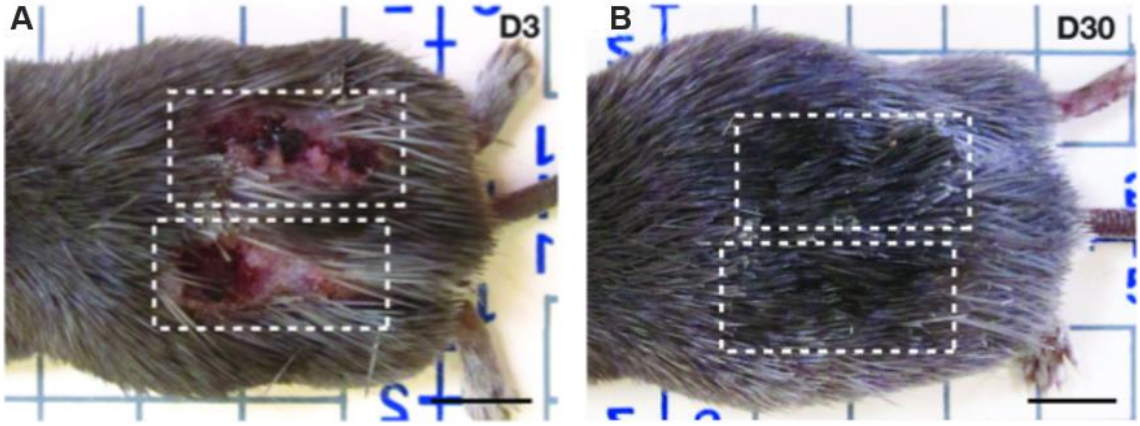

Figure 17 - *Acomys* present skin autotomy and subsequent rapid healing. The same wounds in **A|** are no longer visible at D30 and new spiny hairs cover the damaged area (**B|**). Adapted from [90].

Following these observations, extensive tissue regeneration in the ear was also reported (Figure 18|A) [91, 92]. While it is still not known if other *Acomys* tissues are capable of regeneration, these studies led to believe that this ability may also be extended to the nervous system, since nerve fibers marked by Tuj-1 (Figure 18|B) [91] or peripherin [92] were observed within the regenerated tissue. Additionally RNA-Seq analysis revealed that genes associated with axon guidance, neuroactivity and growth were enriched in *Acomys* epidermis when compared with *Mus* [92].

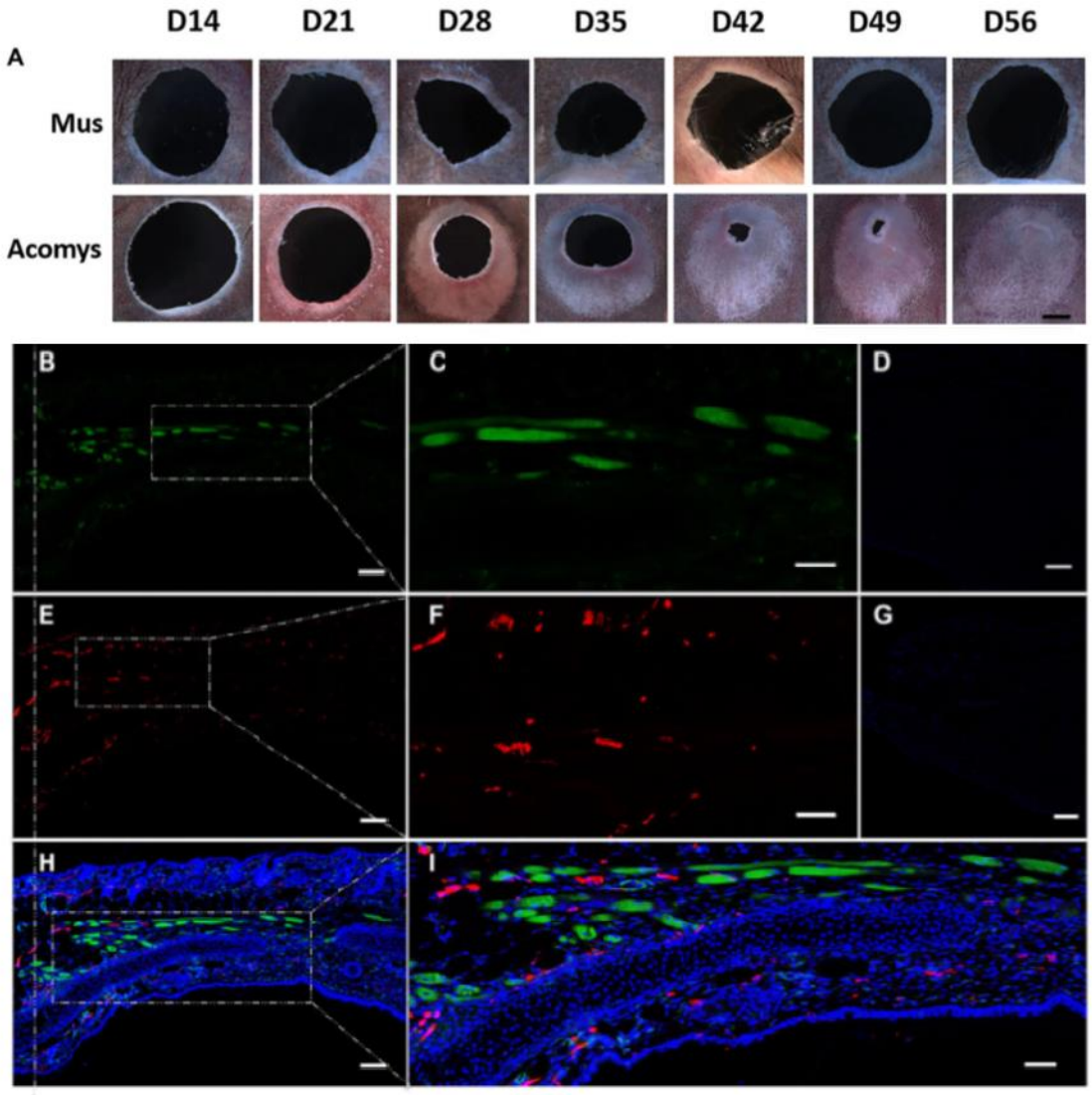

Figure 18 - Ear punch closure of *Acomys cahirinus*. A| Timeline of ear punch closure of *Acomys cahirinus* versus *Mus* C57BL/6 at weekly intervals between day 14 and day 56. Scale bar 1 mm. **B-I|** Immunofluorescence analysis of regenerated *Acomys cahirinus* ear punch. **B|** Incubated with anti-actin (50x). C| Probed with anti-actin (200x). D| Negative control in which the primary antiserum was omitted (200×). E| Incubated with anti-TUJ1 (50x). F| Probed with anti-TUJ1 (200x). G| Negative control stained with secondary antibody only (200x). H| Merge of B+E+Dapi (5x). I| Merge of B+E+Dapi (200x). All scale bars 100 µm. Adapted from [91].

Although axons regenerate in adult *Acomys* after ear injury, CNS regeneration remains unexplored. Studies in this field are of great interest, since the analysis of spinal cord regeneration in a mammal with a high regenerative capacity may provide valuable insights in the spinal cord repair field.

Which unique features underlie *Acomys* regenerative capacity?

Although it is still not known if other *Acomys* tissues are able to regenerate, the reported increased regeneration ability has been associated with decreased fibrosis and scarring as well with a distinct inflammatory response [92].

The ECM regulates many cell processes and is critically important for cell growth, survival, differentiation and morphogenesis. During the wound healing process, this complex structure is constantly being remodeled, which makes it a valuable tool in the regenerative medicine field [93].

During wound healing of fetal and adult wounds, several ECM components can be differently regulated, namely collagens. In fetal wounds there is an upregulation of types III and IV, while type I is downregulated [94]. In *Acomys* skin wounds, collagen type III was found in higher levels than collagen type I, which is predominant in *Mus* wounds, suggesting that *Acomys* wounds are more similar to fetal than to adult wounds. Additionally, the collagen fibers were organized in a more porous structure instead of being densely packed [90]. In ear wounds, lower levels and a later start of collagen deposition were also reported [91, 92]. Since collagen I has been associated with the astrocytic scar formation [95], decreased levels of this protein in *Acomys* ECM could facilitate axon regeneration following spinal cord injury.

Besides lower collagen deposition, the analysis of *Acomys* regenerated ear tissue also revealed an upregulation of the Fn1 and Tnc genes, suggesting that the ECM might be enriched in fibronectin and tenascin. Fibronectin has been reported to support neurite outgrowth [96] and to promote spinal cord regeneration after injury [97, 98]. Identically, tenascin enhances and supports neurite outgrowth [99] and promotes locomotor functional recovery following SCI [100]. This ECM component is expressed by astrocytes and meningeal fibroblasts and its expression is upregulated after CNS injuries [100].

Together, these data suggest that an ECM enriched in tenascin and fibronectin and poor in collagen type I can be correlated with an increased

regenerative ability. Therefore, the different ECM compositions in *Acomys* and *Mus* (Figure 19) suggest that the extracellular environment can be correlated with *Acomys* regenerative ability [92], since it stimulates regeneration over scarring.

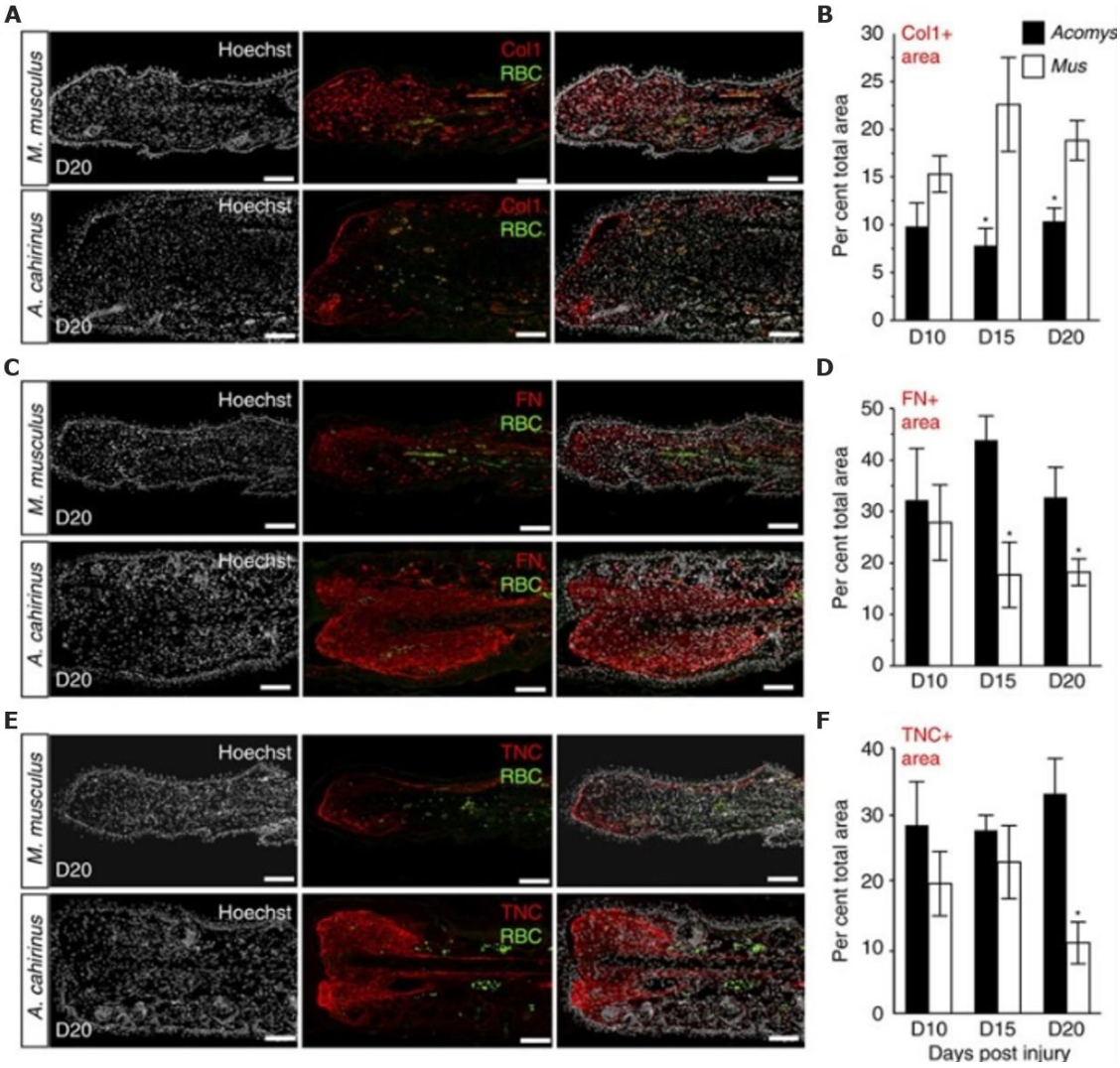

Figure 19 – Immunostaining for the extracellular matrix proteins reveals differences in the total area of protein deposition. A, C, E| Representative images for immunohistochemistry to detect collagen I (A|), fibronectin (C|) and tenascin (E|) in *Mus musculus* and *Acomys cahirinus*. Scale bar, 100 μm. **B, D, F|** To quantify positive signal, a region of interest was created to include tissue distal to the original cartilage and to exclude hair follicles and epidermis. The ratio of total immuno-positive area per total area of the region of interest was calculated. Data represent mean and s.e.m., *t-test $p<0.05$ for *M. musculus* versus *A. cahirinus* comparison for the day indicated. Abbreviations: Col1 – collagen I; FN – fibronectin; TNC – tenascin; RBC – red blood cells. Adapted from [92].

In addition to extensive changes in the ECM composition, *Acomys* also have a quite different inflammatory response when compared to *Mus*. While *Mus* present the typical strong inflammatory response of adult mammal injury, *Acomys* almost do not express cytokines and chemokines in the wound site [101]. In addition, after injury *Mus* upregulate genes involved in inflammatory pathways while *Acomys* upregulate genes involved in tissue remodeling [94]. Similarly to ECM composition, inflammatory response in *Acomys* seems to be comparable to that in fetal wounds. Along with the absence of pro-inflammatory molecules, a strikingly reduced number of macrophages and lymphocytes can contribute to the decreased tissue scarring in *Acomys* [101].

The role of macrophages is not fully understood and it is important to keep in mind that these cells are important for either regeneration or scarring. Depletion of macrophages may result in different outcomes. While it has been shown to lead to reduced fibrosis and to promote axonal growth after injury [102], it was also reported to inhibit regeneration of zebra fish tail [103] and salamander limbs [104]. Importantly, macrophage depletion in *Acomys* ear tissue results in a non-regenerating scenario [105]. It has been hypothesized that macrophages are responsible for the removal of senescent cells that secrete inhibitory factors [105], since the accumulation of senescent cells is reported to impair limb regeneration in salamanders [106]. Although there are some inconsistent results regarding macrophages role in regenerative processes [94, 105], it is well accepted that there is a reduced number of macrophages activated towards a pro-inflammatory phenotype that infiltrate the lesioned area. Different phenotypes may explain the different outcomes that have been reported. Future work focusing in the study of different types of macrophages may elucidate how these can enhance tissue regeneration and whether the injury site may influence the activated types of cells [105].

Preliminary results

In collaboration with The Molecular and Regenerative Medicine Laboratory of Universidade do Algarve, the Nerve Regeneration Group has begun to investigate CNS regeneration in *Acomys cahirinus*.

To investigate CNS regeneration, complete spinal cord injuries were performed in both *Mus* and *Acomys.* The animals were maintained for 12 weeks to assess functional recovery. Locomotor function was evaluated using the Basso Mouse Scale [107] and bladder function recovery was also followed.

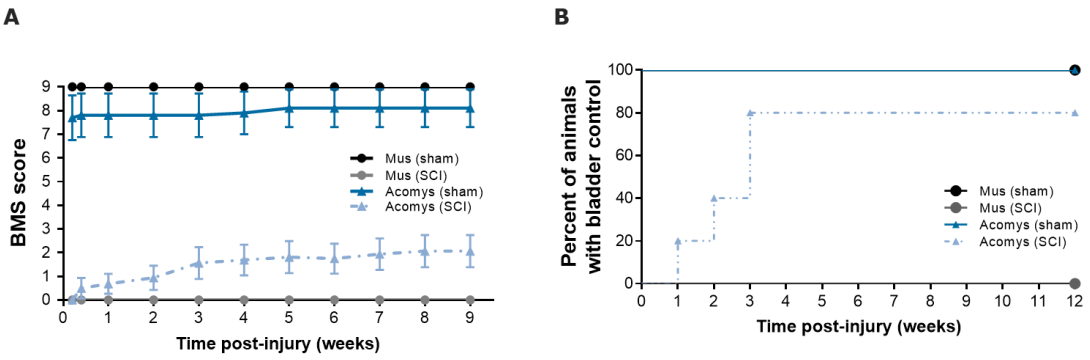

Figure 20 - *Acomys* display functional recovery following spinal cord injury. A| BMS Score. After complete transection of the spinal cord, *Acomys* recover some locomotor function. **B| Bladder Function.** *Acomys* are able to regain bladder control following injury. *Mus* do not recover motor or bladder control. Abbreviations: BMS – Basso Mouse Scale; SCI – Spinal Cord Injury.

As shown in Figure 20, after complete transection of the spinal cord, *Acomys* display some motor recovery (Figure 20|A) and 80% of the animals (Figure 20|B) regain bladder function, unlike *Mus* that do not recover motor or bladder control. Sham-operated animals maintain locomotion and bladder function throughout the experiment.

To determine whether this regenerative response was due to intrinsic factors, neurite outgrowth of DRG neurons from *Acomys* and *Mus* was evaluated in both growth-permissive (laminin) and growth-inhibitory (aggrecan) environments.

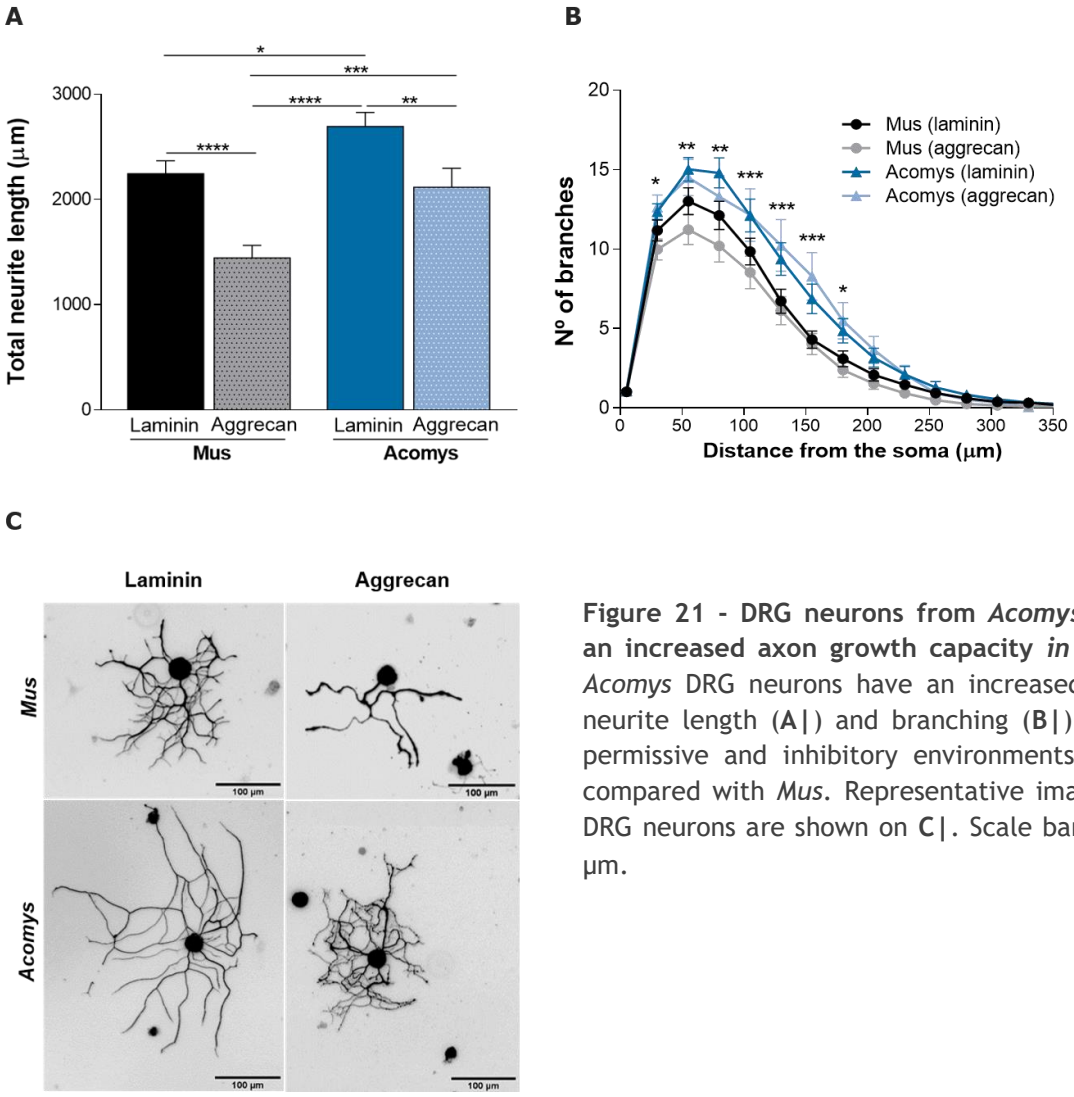

Figure 21 - DRG neurons from *Acomys* have an increased axon growth capacity *in vitro*. *Acomys* DRG neurons have an increased total neurite length (**A|**) and branching (**B|**) under permissive and inhibitory environments when compared with *Mus*. Representative images of DRG neurons are shown on **C|**. Scale bars: 100 µm.

Acomys DRG neurons have an increased total neurite length (Figure 21|A) and branching (Figure 21|B) under permissive and inhibitory conditions when compared with *Mus*, suggesting an increased axon growth capacity and a lower sensitivity to inhibitory factors.

Regarding these remarkable results, the work developed as part of this thesis aimed at analyzing cellular and molecular details of the *Acomys* spinal cord regeneration, hoping it will provide further comprehension of the regenerative mechanisms in vertebrates that may be relevant to the advance of regenerative medicine with possible clinical applications.

II. MATERIALS AND METHODS

1. Spinal Cord Histological Analysis

1.1. Immunohistochemistry (IHC)

50 µm spinal cord longitudinal sections were immunostained, with the exception of the immunohistochemistry against **5-HT**, in which cross-sections were used.

For the **F4/80** immunohistochemistry, previously to the common protocol, samples were incubated for 5 minutes in 0.1% sodium borohydride (NaBoro; Sigma-Aldrich, 452882) in TE pH 9 buffer.

For the **βIII-tubulin** immunohistochemistry, previously to the rest of the protocol, samples were incubated overnight (O/N) at 4°C with 0.1M glycine (Merck Millipore, 1.04201.1000) and for 30 minutes in 1% Triton X-100 (Sigma-Aldrich, T9284) in PBS.

Samples were washed with 0.1M phosphate buffer (PB) and then incubated with 200 mM ammonium chloride (NH4Cl; VWR (Merck), 1.01145.0500) for 30 minutes at room temperature (RT), in order to quench the autofluorescence of the free aldehydes from fixation. In the **βIII-tubulin** immunohistochemistry, after this step samples were incubated for 5 minutes in 0.1% NaBoro in TE pH 9.

Samples were incubated for 1 hour at RT in blocking buffer:

- 10% Donkey Serum (Sigma-Aldrich, 9663) and 0.3% Triton X-100 (Sigma-Aldrich, T9284) in 0.1M PB for the **5-HT** immunohistochemistry

- 5% Fetal Bovine Serum (FBS; Sigma-Aldrich, F9665) and 0.3% Triton X-100 in 0.1M PB for the **Collagen I**, **CSPG**, **CTb**, **F4/80**, **Fibronectin**, **GFAP**, **IBA1**, **SCG10** and **Tenascin** immunohistochemistries

- 1 mg/mL BSA and 1% Triton X-100 in PBS for the **βIII-tubulin** immunohistochemistry

The blocked samples were then incubated with the primary antibody in blocking buffer O/N at 4ºC. The following day, after washing with 0.1M PB, the sections were incubated with the secondary antibody in blocking buffer for 2 hours at RT. Only in the **βIII-tubulin** immunohistochemistry, samples were incubated for 48 hours with the primary antibody and 48 hours with the secondary antibody. All primary and secondary antibodies are described in table 1 and table 2.

Table 1 - Primary Antibodies used in the immunohistochemistries

Primary Antibodies		Dilution	Host
Anti - **5-HT**	ImmunoStar, 20080	1:10 000	Rabbit
Anti - **Collagen I**	Rockland, 600-401-103-0.1	1:200	Rabbit
Anti - **CSGP**	Sigma, C8035	1:1000	Mouse
Anti - **CTb**	List Biological Laboratories, 703	1:30 000	Goat
Anti - **F4/80**	Bio-rad, MCA497	1:20	Rat
Anti - **Fibronectin**	Sigma, F3648	1:200	Rabbit
Anti - **GFAP**	Dako, Z0334	1:2000	Rabbit
Anti - **IBA1**	Synaptic Systems, 234013	1:2000	Rabbit
Anti - **SCG10**	Novus Biologicals, NBP1-49461	1:5000	Rabbit
Anti - **Tenascin**	Non commercial	1:100	Rat
Anti - **βIII-tubulin**	Promega, G7121	1:500	Mouse

Since in the **CTb** immunohistochemistry the secondary antibody is biotinylated, the samples were then incubated for 1 hour with Streptavidin, Alexa Fluor® 568 Conjugate (Thermo Fisher Scientific, S-11226) 1:1000 in TBS-T.

Sections were mounted in PB 0.1M and air dried before coverslipping with Vectashield with DAPI (LINARIS Biologische Produkte GmbH, H-1200). Image acquisition was performed using the motorized upright epifluorescence microscope Zeiss Axio Imager Z1.

Table 2 - Secondary Antibodies used in the immunohistochemistries

Primary Antibody	SecondaryAntibody	Dilution
Anti - **5-HT**	Alexa Fluor® 568 AffiniPure Donkey Anti-Rabbit Life Technologies, A10042	1:1000
Anti - **CSPG**	Alexa Fluor® 488 AffiniPure Donkey Anti-Mouse Life Technologies, A21202	1:1000
Anti – **CTb**	Biotinylated Horse Anti-Goat IgG (H+L) Vector Laboratories, BA9500 Streptavidin, Alexa Fluor® 568 Conjugate Thermo Fisher Scientific, S-11226	1:2000 1:1000
Anti - **GFAP**	Alexa Fluor® 488 AffiniPure Donkey Anti-Rabbit Life Technologies, A21206	1:1000
Anti - **Collagen** Anti - **Fibronectin** Anti – **IBA1** Anti – **SCG10**	Alexa Fluor® 488 AffiniPure Goat Anti-Rabbit IgG (H+L) Jackson ImmunoResearch Europe, 111-545-003	1:1000
Anti – **F4/80** Anti – **Tenascin**	Alexa Fluor® 568 AffiniPure Goat Anti-Rat Life Technologies, A11077	1:1000
Anti – **βIII-tubulin**	Alexa Fluor® 488 AffiniPure Goat Anti-Mouse IgG Jackson ImmunoResearch Laboratories, 115-545-003	1:500

1.2. Masson's Trichrome Staining

10 µm cryosections from PFA fixed spinal cords were stained with Masson's Trichrome (Sigma-Aldrich, Kit HT15).

Briefly, after 1 hour at RT in Bouin solution (VWR, 7000.100), sections were left for 5 minutes in Celestine Blue, 5 minutes in Gill's Hematoxylin and 5 minutes in Briebrich Scarlet-Acid Fuchsin. In between stainings sections were washed with distilled water. After 5 minutes in "work solution" (one time Phosphomolybdic Acid Solution, one time Phosphotungstic Acid Solution and two times distilled water), samples were left for 5 minutes in Anillin Blue and 3 minutes in 1% acetic acid. Samples were washed with distilled water and, after a few hours dehydrating, mounted in DPX.

2. Functional Evaluation following Spinal Cord Injury

2.1. Animals

Animals were bred with *ad libitum* access to water and rodent food, supplemented with seeds and fresh fruit, and were kept on a 12 hour light and dark cycle. All mice were handled and euthanized according to the i3S humane endpoints standard operation procedure established according to FELASA's recommendations (www.felasa.eu).

Spinal cord injuries were performed by complete transection at T8 and *Acomys* were maintained for 8 weeks to assess motor function recovery using the Basso mouse score (BMS) and bladder function improvement.

2.2. Functional Evaluation

In the weeks preceding the surgery, all of animals were habituated to the open-field arena in two separate 10 minutes sessions. The von Frey filaments test and urine spot test were also performed twice in order to establish baseline values.

2.2.1. Urine Spot Test

Animals were left on top of filter paper for 30 minutes and urine spots were detected using ultraviolet illumination of the Gel-Doc-XR (Bio-Rad).

2.2.2. Open Field Locomotion

The Basso Mouse Scale (BMS) was developed to examine open-field locomotion in spinal cord injured mice [107] and has become widely used in mouse functional testing research as an indicator of recovery. This test evaluates different locomotor categories such as paralysis, weight support, and stepping.

Animals were put in an open-field and a score was attributed by two observers to both right and left hind limbs. Definitions of each score are shown in Table 3.

Table 3 - Scores for the Basso Mouse Scale for Locomotion. Adapted from [108]

Score	
0	No ankle movement
1	Slight ankle movement
2	Extensive ankle movement
3	Plantar placing of the paw with or without weight support -OR- Occasional, frequent or consistent dorsal stepping but no plantar stepping
4	Occasional plantar stepping
5	Frequent or consistent plantar stepping, no coordination -OR- Frequent or consistent plantar stepping, *some* coordination, paws *rotated* at initial contact and lift off (R/R)
6	Frequent or consistent plantar stepping, *some* coordination, paws *parallel* at initial contact (P/R, P/P) -OR- Frequent or consistent plantar stepping, *mostly* coordinated, paws *rotated* at initial contact and lift off (R/R)
7	Frequent or consistent plantar stepping, *mostly* coordinated, paws *parallel* at initial contact and *rotated* at lift off (P/R) -OR- Frequent or consistent plantar stepping, *mostly* coordinated, paws *parallel* at initial contact and lift off (P/P), and *severe* trunk instability
8	Frequent or consistent plantar stepping, *mostly* coordinated, paws *parallel* at initial contact and lift off (P/P), and *mild* trunk instability -OR- Frequent or consistent plantar stepping, *mostly* coordinated, paws *parallel* at initial contact and lift off (P/P), and *normal* trunk stability and tail *down or up* & *down*
9	Frequent or consistent plantar stepping, *mostly* coordinated, paws *parallel* at initial contact and lift off (P/P), and *normal* trunk stability and tail *always* up.

2.2.3. von Frey Filament Test

Rodents exhibit a paw withdrawal reflex when the paw is unexpectedly touched. The animal indicates sensation by pulling back its paw. Touch sensitivity is assessed with von Frey filaments. These filaments are applied to the underside of the paw after the mouse has settled into a comfortable position within a restricted area that has a perforated floor. The filaments are calibrated to flex when the set force is applied to the paw. Filaments are presented in order of increasing stiffness, until a paw withdrawal is detected. The animal is tested again with the same filament as well as the filament just below that which elicited an initial response to insure correct identification of minimal required force to elicit a response.

III. Results and Discussion

Part of the results reported in this section were included in a poster presented at the Glasgow 2018 Neurotrauma Summer School, jointly organized by Wings for Life and International Spinal Research Trust: "The African Spiny Mouse regenerates after complete spinal cord injury".

Acomys injured spinal cord presents reduced fibrosis

Histological analysis of the spinal cord of animals following spinal cord injury may be a valuable tool to elucidate how *Acomys* regenerative capacity arises. Our first analysis focused on labelling the glial scar, using antibodies against either GFAP or CSPG.

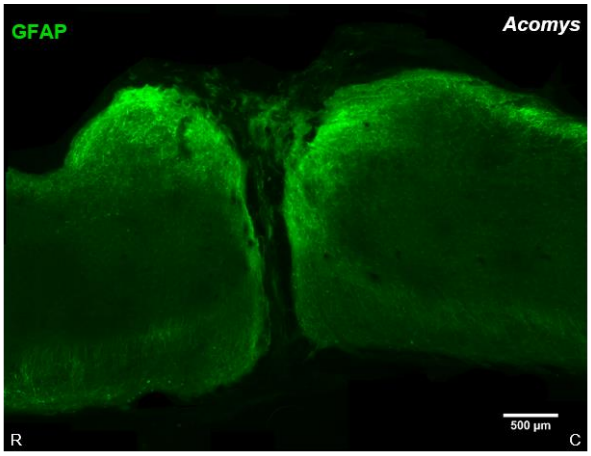

Figure 22 - Histological spinal cord section of *Acomys* labelled for GFAP. Similar to *Mus*, after injury, *Acomys* spinal cord presents increased expression of GFAP with local astrocyte activation. Scale bar: 500 µm. Abbreviations: GFAP – Glial Fibrillary Acidic Protein; R – Rostral; C – Caudal.

Unlike the IHC against GFAP (Figure 22), the IHC targeting CSPG did not result in a specific staining. Since there are no antibodies produced in *Acomys*, there is no guarantee that a specific antibody will recognize its target in this species. Using antibodies from different hosts and finding which ones work in *Acomys* and which ones don't is a possible approach to try to circumvent this problem, as it will be further discussed.

Staining with GFAP, presented in Figure 22, proves that, similarly to *Mus*, after injury, *Acomys* spinal cord presents increased expression of GFAP with local astrocyte activation, isolating the lesion site. This exclusion of the lesion site has a beneficial effect since it minimizes the inflammatory response and cellular degeneration [14, 16]. However, the strong inflammatory response around the lesion results in fibrosis, which is one of the causes for the failure of regeneration. The regenerative capacity of *Acomys* has been associated with a decreased fibrosis [92].

To assess this decreased formation of fibrotic tissue, we performed a Masson's trichrome staining in the injured spinal cords. The principle of this staining protocol is that muscle and collagen fibers stain differentially when treated sequentially with Biebrich Scarlet-Acid Fuchsin, PTA/PMA and Aniline Blue. Cytoplasm and muscle fibers stain red whereas collagen displays blue coloration. Since collagen deposition is a hallmark of fibrosis, this coloration allows a visual perception of fibrosis in the injured tissue.

As depicted in Figure 23, at 12 weeks after injury, *Mus* spinal cord presents a much higher collagen deposition (fibrotic scarring) than *Acomys*, in which collagen accumulates in much lower levels, indicating a reduced fibrosis. These findings are consistent with previous studies reporting reduced fibrosis as a probable cause for *Acomys* remarkable regenerative capacity [92].

Although we assessed that in fact there is a reduced formation of fibrotic tissue, none of these findings prove that *Acomys* axons are regeneration-competent.

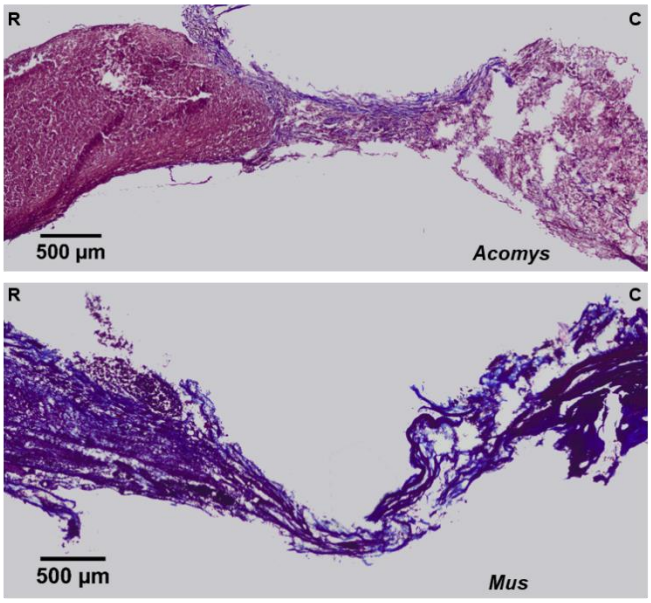

Figure 23 - Histological spinal cord sections of *Acomys* and *Mus* stained with Masson's Trichrome staining. *Acomys* spinal cord exhibits lower collagen deposition, indicating a reduced fibrosis, when compared with *Mus* in which collagen is accumulated at higher levels (fibrotic scarring) at 12 weeks after injury. Scale bar: 500 µm. Abbreviations: R – Rostral; C – Caudal.

Acomys descending axons are able to cross the glial scar

To understand if *Acomys'* axons are able to regenerate or not, we used two different stainings of spinal cord tracts.

Cholera toxin subunit B (CTb) is a neuroanatomical retrograde tracer which had been injected in the animals' sciatic nerve prior to sacrifice. Using an anti-CTb antibody allows the visualization of the dorsal column tract. This ascending tract is interrupted when a complete transection of the spinal cord is performed and, for that reason, CTb labelled axons found rostrally to the lesion site would indicate that axonal regeneration is taking place. However, we did not find any, as depicted in Figure 24.

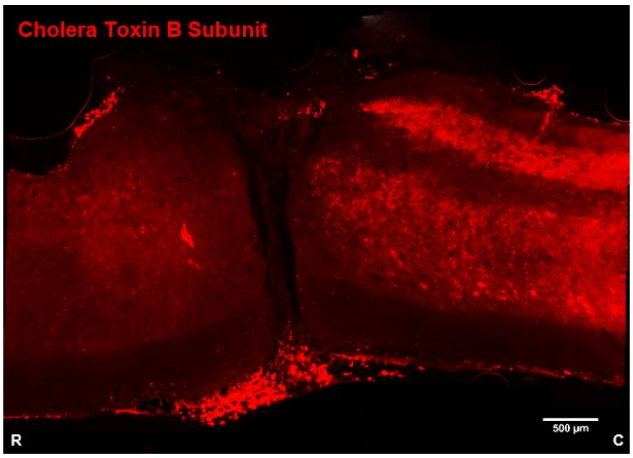

Figure 24 - Histological spinal cord section of *Acomys* labelled for Cholera Toxin Subunit B. CTb-labelled ascending axons are not able to regenerate rostrally to the lesion site. Scale bars: 500 µm. Abbreviations: R – rostral; C – caudal.

5-hydroxytryptamine, or serotonin, is a neurotransmitter that plays an important role in modulating the activity of spinal networks involved in vertebrate locomotion.

An immunohistochemistry against 5-HT was performed in spinal cord cross-sections located both rostrally and caudally to the lesion site (Figure 25). Serotonin staining is observed caudally (Figure 25|B) to the lesion site. Since the descendent tract along which the serotonergic axons run, the raphespinal tract, is interrupted when a complete transection is performed, the presence of these axons caudally to the lesion site shows that *Acomys* descending serotonergic axons might have the capacity to cross the glial scar.

It has been reported that changes in the serotonergic system can produce varying degrees of locomotor dysfunction through to paralysis. To date, various approaches targeting the different components of the serotonergic system have been employed to restore limb coordination and improve locomotor function in experimental models of SCI [108]. Therefore, the hypothesis that *Acomys* serotonergic axons are able to cross the glial scar is consistent with the preliminary results which refer to the striking functional recovery following spinal cord injury (Figure 20, Figure 21).

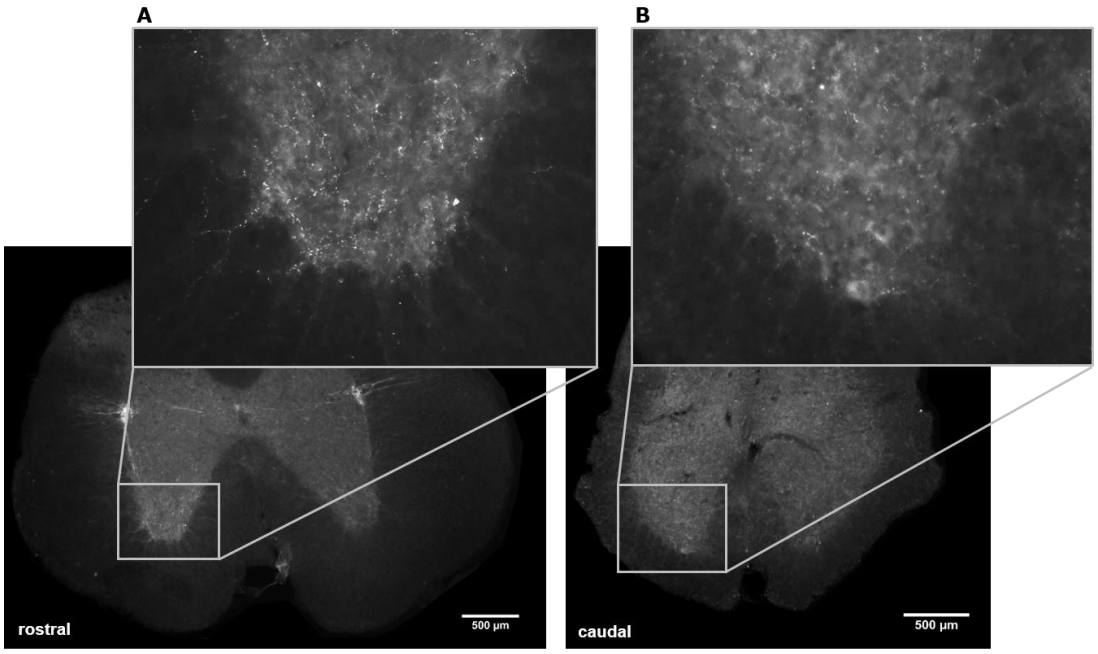

Figure 25 - *Acomys* descending serotonergic axons have the ability to cross the glial scar following injury. Serotonin staining is observed caudally (**B|**) to the lesion site. Scale bar = 500 µm.

Antibodies from different host species enable the immunostaining of *Acomys* regenerating axons and extracellular matrix

As previously described, there are no antibodies that are totally specific to *Acomys*. Hence, part of the work developed in this thesis aimed at finding antibodies that could efficiently label different targets of interest for future studies.

Besides labelling regenerating axons, it is of interest to find ways of staining elements of the extracellular matrix or that constitute part of the immune response seen after spinal cord injury, since these are thought to be the unique features underlying *Acomys* regenerative ability [92].

Starting with immunostaining of regenerating axons, two different protocols were tested: a stain for βIII-tubulin, which is widely used as a neuron-specific marker [109], and another targeting SCG10, a selective marker for injured regenerating sensory axons of the dorsal column tract [110]. In both IHC there was a successful marking of axons around the lesion site of injured spinal cords. Representative images are shown in Figure 26.

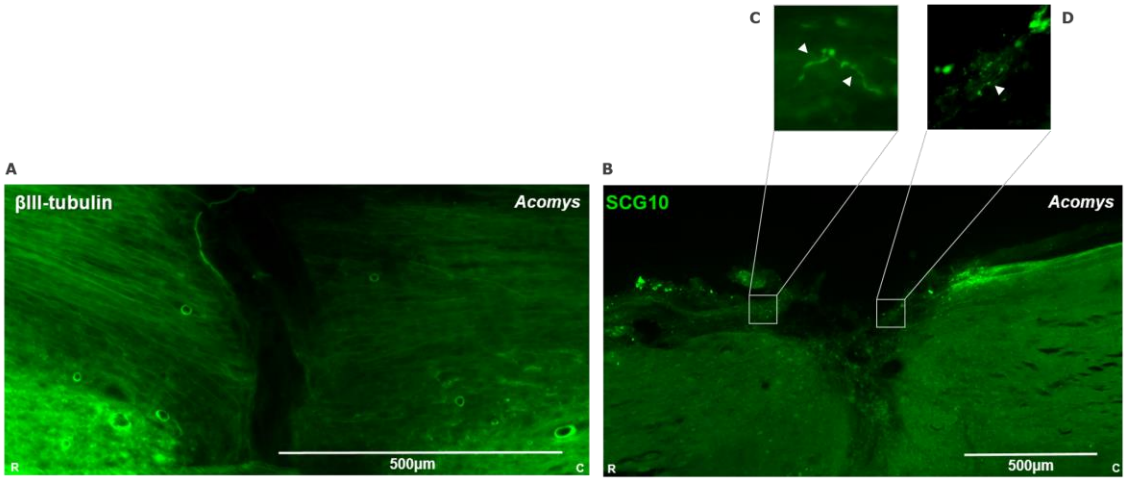

Figure 26 - Histological spinal cord sections of *Acomys* labelled for βIII-tubulin and SCG10. A| βIII-tubulin. There are no visible axons crossing the lesion site. **B| SCG10.** There are regenerating axons on both sides of the lesion (white arrows, **C|** and **D|**). Scale bars: 500 µm. Abbreviations: R – Rostral; C – Caudal.

Although there were no visible axons crossing the lesion site in this section of the spinal cord, the βIII-tubulin IHC resulted in an efficient labelling axons (Figure 26|A), which was our main goal. A single spinal cord was used to test several antibodies; in the future, in order to make conclusions, it is necessary to stain a whole spinal cord against a certain antibody of interest. Regarding the SCG10 IHC (Figure 26|B), despite the elevated levels of background fluorescence, it is possible to see regenerating axons both caudally and rostrally to the lesion site (Figure 26|C and 26|D). As an attempt of optimizing the protocol and reduce the background fluorescence, 5 minutes of incubation with NaBoro before the rest of the protocol were added. However, the results did not differ from the ones previously obtained.

Regarding the immunostaining of the extracellular matrix, our main goal was to achieve staining of collagen I, tenascin and fibronectin, the components reported to be differentially expressed in *Acomys* and *Mus* extracellular matrices [92]. The only antibody which was able to efficiently mark the spinal cord sections was the one against collagen type I. As depicted in Figure 27, the signal was very strong and particularly high at the lesion site, as it would be expected.

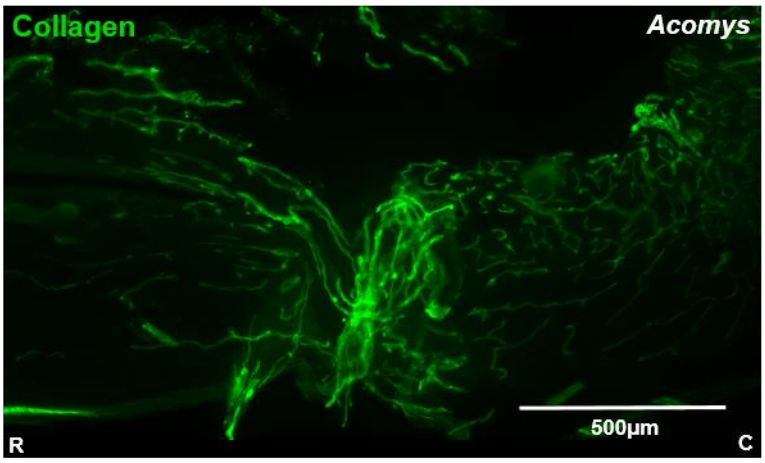

Figure 27 - Histological spinal cord section of *Acomys* labelled for Collagen I. After injury, *Acomys* spinal cord presents increased expression of collagen in the lesion site. Scale bar 500 µm. Abbreviations: R – Rostral; C – Caudal.

Although here we only tested collagen type I, further work could include selective stainings for other types, such as collagen type III, since the ratio of these types in *Acomys* seems to differ from the one reported in *Mus* [90] and to be closer to the one found in fetal wounds [94].

Lastly, antibodies against IBA1 and F4/80 were tested as an attempt to identify cells involved in the inflammatory response in the injured spinal cord. IBA1 is marker for microglia [111] and F4/80 marks macrophages [112]. Only the anti-IBA1 antibody was successful in recognizing its target in *Acomys* spinal cord. As shown in Figure 28|B, it was possible to observe "star" shaped cells using a higher magnification objective.

In the future, more strategies aiming at the visualization of cells involved in the immune response, focusing specifically in the study of different phenotypes of macrophages should be developed. These may elucidate how differently activated macrophages can enhance tissue regeneration and whether the injury site has an influence in the activated cell types [105].

All the performed immunohistochemistries had the purpose of assessing what kind of stainings would be possible to obtain in *Acomys* spinal cords. In order to adequately use this approach to study regeneration

in *Acomys*, the same stainings will have to be performed in *Mus* spinal cord sections, to be used as a control and in order to allow the perception of the differences existent between species.

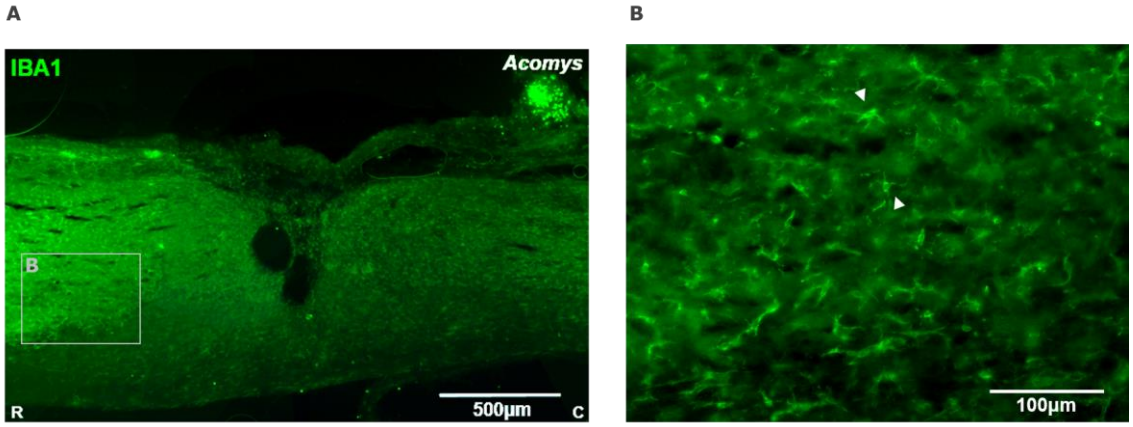

Figure 28 - Histological spinal cord section of *Acomys* labelled for IBA1. A| 10x objective. IBA1 efficiently stained the spinal cord section. Scale bar: 500 µm. **B| 20x objective**. Using a higher magnification it is possible to visualize "star" shaped cells, indicated by the white arrows. Scale bar: 100 µm. Abbreviations: R – Rostral; C – Caudal.

Even though these findings reveal that it is possible to visualize a variety of targets, we are still looking to discover new antibodies that can efficiently stain histological sections. Regarding fibronectin and tenascin, we intent to repeat the experiment with different antibodies. Relatively to macrophages, our next test will be an antibody against CD68, a protein highly expressed by cells in the monocyte lineage, as macrophages and other mononuclear phagocytes [113].

Acomys recover motor and bladder function after complete transection of the spinal cord

In order to validate the previously obtained results regarding the functional evaluation following spinal cord injury, the experiment is currently being repeated. Complete transection of the spinal cord was performed and functional recovery of animals is being assessed for 8 weeks post-injury. Although the evaluation is not complete, there are already some promising results. Additionally, it is important to emphasize that this

experiment allowed us to better understand details about the husbandry of these animals and their handling, since it is the first time this species is bred at the i3S animal facility.

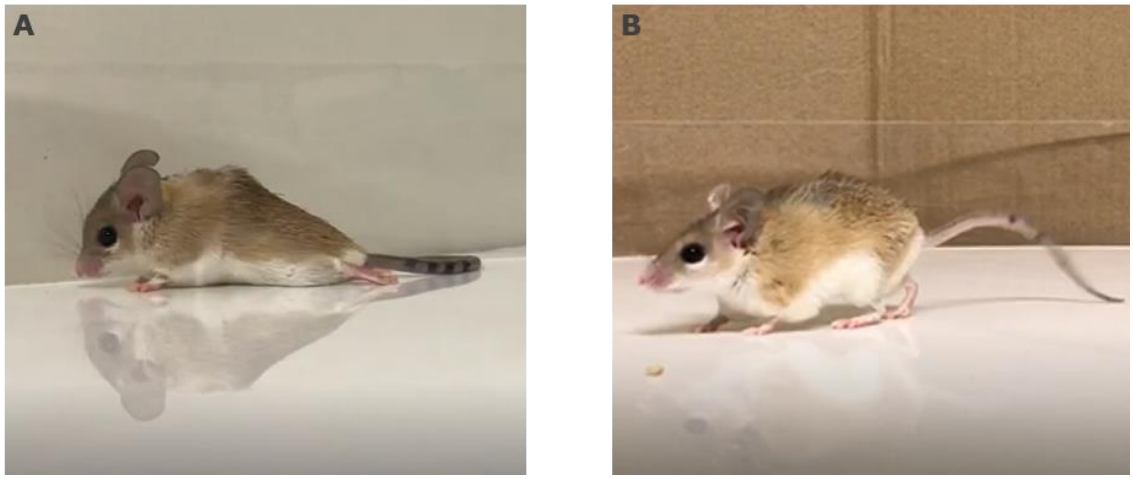

Figure 29 - Locomotor Function Recovery in *Acomys*. Representative frames of open field locomotion videos. **A| 2 days post-injury**. Absence of ankle movement, BMS score 0. **B| 5 weeks post-injury.** Weight supported plantar stepping, BMS score 4.

Regarding the locomotor function, the results resemble the ones previously reported. As seen in Figure 20|A of the Preliminary Results section, BMS scores showed that *Acomys* are able to regain some function following spinal cord injury, since their scores start at zero and increase from there, until an average score of 2 or 3. Although these scores still fall short of the ones obtained by *Acomys* of the sham group, a clear improvement is noticed. This time repeating the experience, at 5 weeks post injury, we started seeing animals with weight support, which translates in a BMS score of 4 (Figure 29). At this point, it is possible to start the evaluation of sensitivity with the von Frey filaments test. Regarding this test, we recently established that baseline values for *Acomys* evidence that they feel less than *Mus*, since filaments with a higher diameter are needed in order to cause paw withdrawal.

This consideration about baseline values is also needed when evaluating BMS scores. The scores obtained by *Acomys* of the sham group are not as high and are more variable than the ones obtained by *Mus* of the sham group (Figure 20|A). This suggests that the scale used to evaluate *Acomys* movement may not be totally adequate and it is possibly lowering

the scores due to specific manners of this species. It is necessary to consider all of these factors when comparing functional results of *Acomys* and *Mus*.

Another parameter evaluated to assess functional recovery was bladder control. Manual bladder voiding of the animals was carried out twice a day in the weeks following the surgeries, until it was understandable that bladders were empty before the manual voiding. Accordingly with previous results (Figure 20|B), in which 80% of the animals had regained bladder function, 100% of the animals in the new experience were also able to regain bladder control.

Lastly, we are addressing a new test to evaluate urinary function: the urine spot test. The animals are left in filter paper during 30 minutes and the resulting urine spots are imaged [114]. We are hoping that the joint interpretation of the results of this voiding assay and further histological analysis of the bladders will allow us to prove that *Acomys* are in fact regaining bladder function, excluding the possibility that they are incontinent.

Altogether, our new results are very consistent with the ones previously obtained and keep pointing to *Acomys* as an extremely valuable model for studies in the spinal cord regeneration field, due to its capacity of functional recovery after spinal cord injury.

IV. CONCLUSIONS AND FUTURE PERSPECTIVES

Mammals generally do not regenerate as they respond to wounding with scarring, the main cause of their limited regenerative capacity. However, *Acomys* have recently been described as potential regenerator mammals, being for that reason a useful model to further comprehend regenerative mechanisms in vertebrates that may be relevant to advance regenerative medicine with possible clinical applications. Our main goal was to explore spinal cord regeneration in *Acomys cahirinus*, aiming to provide valuable insights into the spinal cord regeneration field.

Here we report that *Acomys* recover both motor and bladder function following complete transection of the spinal cord. Additionally, histological analysis of the injured spinal cords revealed that these present reduced fibrosis and that *Acomys* descending serotonergic axons are able to cross the glial scar.

Even though these results are promising, further work is needed to perceive the mechanisms underlying *Acomys* striking regenerative capacity. Histological analysis is a useful tool to compare the extracellular matrix and the cells involved in the immune response in *Acomys* and *Mus*, which are unable to regenerate. Additionally, studies to assess if *Acomys* neurons present an increased outgrowth *in vivo* as they do *in vitro* may also be of interest. Finally, identifying candidate regeneration-related genes or even molecules driving the healing of a spinal cord injury would be notable and a great step forward in the search of strategies translatable into clinical applications.

Chapter 5

Main Conclusions and Future Perspectives

The Edwin Smith papyrus, an ancient Egyptian physician textbook and the world's oldest known surgical document, described spinal cord injuries as an "ailment not to be treated" [115]. Although this is the oldest known document on spinal injuries, over 3000 years later treatments for this disability remain largely palliative instead of curative. Despite the continuous research on new possible treatments there are still no fully restorative treatments and, therefore, there is a major need to identify new strategies to repair the injured spinal cord [4].

The main reason why paralysis and loss of sensation are permanent in conditions such as spinal cord injury is the failure of CNS axons regeneration. The limited ability for regeneration is a consequence of the highly inhibitory environment at the injury site and of the failure of central axons in mounting a pro-regenerative program.

Our main goal was to identify New Molecules and New Mechanisms that could promote axon regeneration following spinal cord injury. Although more work is needed to understand the mechanism of action of ACY-738, this drug was able to rescue a degenerative phenotype and shows promise as a New Molecule. Our findings also show that *Acomys* constitute a useful model to unravel mechanisms that may be relevant in the regenerative medicine field.

Altogether, our results show promise as the first steps in meeting the major medical need of developing new treatments for spinal cord injury, changing the paradigm from palliation to more curative interventions.

References

1. International perspectives on spinal cord injury. Malta: World Health Organization; **2013**

2. Singh, A., Tetreault, L., Kalsi-Ryan, S., Nouri, A., & Fehlings, M. G. (**2014**). Global Prevalence and incidence of traumatic spinal cord injury. *Clinical Epidemiology*. https://doi.org/10.2147/CLEP.S68889

3. National Spinal Cord Injury Statistics Center. (**2018**). Spinal Cord Injury Facts and Figures at a Glance.

4. Silva, N. A., Sousa, N., Reis, R. L., & Salgado, A. J. (**2014**). From basics to clinical: A comprehensive review on spinal cord injury. *Progress in Neurobiology.* https://doi.org/10.1016/j.pneurobio.2013.11.002

5. Martini, Frederic, Michael J. Timmons, and Robert B. Tallitsch. Human Anatomy. 7th edition. **2011.** Upper Saddle River, N.J: Prentice Hall,

6. Sunkel, C. and C. Azevedo, Biologia Molecular e Celular. 5ª edição ed. **2012**, Lisboa: LIDEL

7. Barnes, A. P., & Polleux, F. (**2009**). Establishment of Axon-Dendrite Polarity in Developing Neurons. *Annual Review of Neuroscience*, 32(1), 347–381. https://doi.org/10.1146/annurev.neuro.31.060407.125536

8. Bradke, F., & Dotti, C. C. (**1999**). The role of local actin instability in axon formation. *Science*, 283(5409), 1931–1934. https://doi.org/10.1126/science.283.5409.1931

9. Witte, H., & Bradke, F. (**2008**). The role of the cytoskeleton during neuronal polarization. *Current Opinion in Neurobiology*, https://doi.org/10.1016/j.conb.2008.09.019

10. Cai, D., Qiu, J., Cao, Z., McAtee, M., Bregman, B. S., & Filbin, M. T. (**2001**). Neuronal cyclic AMP controls the developmental loss in ability of axons to regenerate. *The Journal of Neuroscience: The Official Journal of the Society for Neuroscience*, 21(13), 4731–4739. https://doi.org/21/13/4731

11. Ramon y Cajal, S. (**1928**). Degeneration and regeneration of the nervous system. *London, Oxford University Press, Humphrey Milford*

12. Gaudet, A. D., Popovich, P. G., & Ramer, M. S. (**2011**). Wallerian degeneration: Gaining perspective on inflammatory events after peripheral nerve injury. *Journal of Neuroinflammation*, 8, 1–13. https://doi.org/10.1186/1742-2094-8-110

13. Friedman, B., & Aguayo, A. (**1985**). Injured neurons in the olfactory bulb of the adult rat grow axons along grafts of peripheral nerve. *The Journal of Neuroscience*, 5(6), 1616–1625. Retrieved from http://www.jneurosci.org/content/5/6/1616.short

14. Huebner, E. a, & Strittmatter, S. M. (**2009**). Axon Regeneration in the Peripheral and Central Nervous Systems. *Results and Problems in Cell Differentiation*, 48, 339–351. https://doi.org/10.1007/400

15. Schwab, M. E., & Thoenen, H. (**1985**). Dissociated neurons regenerate into sciatic but not optic nerve explants in culture irrespective of neurotrophic factors. *The Journal of Neuroscience: The Official Journal of the Society for Neuroscience*, 5(9), 2415–2423. Retrieved from http://www.ncbi.nlm.nih.gov/pubmed/4032004

16. Silver, J., & Miller, J. H. (**2004**). Regeneration beyond the glial scar. *Nature Reviews Neuroscience*, 5(2), 146–156. https://doi.org/10.1038/nrn1326

17. Eng, L. F. (**1985**). Glial fibrillary acidic protein (GFAP): the major protein of glial intermediate filaments in differentiated astrocytes. *Journal of Neuroimmunology*, 8(C), 203–214. https://doi.org/10.1016/S0165-5728(85)80063-1

18. McKeon, R. J., Schreiber, R. C., Rudge, J. S., & Silver, J. (**1991**). Reduction of Neurite Outgrowth in a Model of Glial Scarring Following CNS Injury Is Correlated With the Expression of Inhibitory Molecules on Reactive Astrocytes. *Journal of Neuroscience*, 11(11), 3398–3411. https://doi.org/10.1523/JNEUROSCI.11-11-03398.1991

19. Morgenstern, D. A., Asher, R. A., & Fawcett, J. W. (**2002**). Chondroitin sulphate proteoglycans in the CNS injury response. *Progress in Brain Research*, 137, 313–332. https://doi.org/10.1016/S0079-6123(02)37024-9

20. Jones, L. L., Margolis, R. U., & Tuszynski, M. H. (**2003**). The chondroitin sulfate proteoglycans neurocan, brevican, phosphacan, and versican are differentially regulated following spinal cord injury. *Experimental Neurology,* 182(2), 399–411. https://doi.org/10.1016/S0014-4886(03)00087-6

21. Snow, D. M., Lemmon, V., Carrino, D. A., Caplan, A. I., & Silver, J. (**1990**). Sulfated proteoglycans in astroglial barriers inhibit neurite outgrowth in vitro.

Experimental Neurology, 109(1), 111–130. https://doi.org/10.1016/S0014-4886(05)80013-5

22. Hynds, D. L., & Snow, D. M. (**1999**). Neurite outgrowth inhibition by chondroitin sulfate proteoglycan: Stalling/stopping exceeds turning in human neuroblastoma growth cones. *Experimental Neurology,* 160(1), 244–255. https://doi.org/10.1006/exnr.1999.7212

23. Lee, J. K., Geoffroy, C. G., Chan, A. F., Tolentino, K. E., Crawford, M. J., Leal, M. A., … Zheng, B. (**2010**). Assessing Spinal Axon Regeneration and Sprouting in Nogo-, MAG-, and OMgp-Deficient Mice. *Neuron*, 66(5), 663–670. https://doi.org/10.1016/j.neuron.2010.05.002

24. Mandolesi, G., Madeddu, F., Bozzi, Y., Maffei, L., & Ratto, G. M. (**2004**). Acute physiological response of mammalian central neurons to axotomy: ionic regulation and electrical activity. *The FASEB Journal*, 18(15), 1934–1936. https://doi.org/10.1096/fj.04-1805fje

25. Sun, F., & He, Z. (**2010**). Neuronal intrinsic barriers for axon regeneration in the adult CNS. *Current Opinion in Neurobiology*. https://doi.org/10.1016/j.conb.2010.03.013

26. Neumann, S., & Woolf, C. J. (**1999**). Regeneration of dorsal column fibers into and beyond the lesion site following adult spinal cord injury. *Neuron*, 23(1), 83–91. https://doi.org/10.1016/S0896-6273(00)80755-2

27. Fletcher, D. A., & Mullins, R. D. (**2010**). Cell mechanics and the cytoskeleton. *Nature*. https://doi.org/10.1038/nature08908

28. Coles, C. H., & Bradke, F. (**2015**). Coordinating Neuronal Actin-Microtubule Dynamics. *Current Biology*. https://doi.org/10.1016/j.cub.2015.06.020

29. Hirokawa, N., Niwa, S., & Tanaka, Y. (**2010**). Molecular motors in neurons: transport mechanisms and roles in brain function, development, and disease. *Neuron*, 68(4), 610–638. https://doi.org/10.1016/j.neuron.2010.09.039

30. Mitchison, T., & Kirschner, M. (**1984**). Dynamic instability of microtubule growth. *Nature*, 312(5991), 237–242. https://doi.org/10.1038/312237a0

31. Kapitein, L. C., & Hoogenraad, C. C. (**2015**). Building the Neuronal Microtubule Cytoskeleton. *Neuron*. https://doi.org/10.1016/j.neuron.2015.05.046

32. Howard, J., & Hyman, A. A. (**2009**). Growth, fluctuation and switching at microtubule plus ends. *Nature Reviews Molecular Cell Biology*. https://doi.org/10.1038/nrm2713

33. Akhmanova, A., & Steinmetz, M. O. (**2008**). Tracking the ends: A dynamic protein network controls the fate of microtubule tips. *Nature Reviews Molecular Cell Biology*. https://doi.org/10.1038/nrm2369

34. Nakagawa, H., Koyama, K., Murata, Y., Morito, M., Akiyama, T., & Nakamura, Y. (**2000**). EB3, a novel member of the EB1 family preferentially expressed in the central nervous system, binds to a CNS-specific APC homologue. *Oncogene*, 19(2), 210–216. https://doi.org/10.1038/sj.onc.1203308

35. Kleele, T., Marinković, P., Williams, P. R., Stern, S., Weigand, E. E., Engerer, P., Misgeld, T. (**2014**). An assay to image neuronal microtubule dynamics in mice. *Nature Communications*, 5. https://doi.org/10.1038/ncomms5827

36. Stepanova, T., Slemmer, J., Hoogenraad, C. C., Lansbergen, G., Dortland, B., De Zeeuw, C. I., Galjart, N. (**2003**). Visualization of microtubule growth in cultured neurons via the use of EB3-GFP (end-binding protein 3-green fluorescent protein). *The Journal of Neuroscience: The Official Journal of the Society for Neuroscience*, 23(7), 2655–2664. https://doi.org/23/7/2655

37. Blanquie, O., & Bradke, F. (**2018**). Cytoskeleton dynamics in axon regeneration. *Current Opinion in Neurobiology*. https://doi.org/10.1016/j.conb.2018.02.024

38. Bradke, F., Fawcett, J. W., & Spira, M. E. (**2012**). Assembly of a new growth cone after axotomy: The precursor to axon regeneration. *Nature Reviews Neuroscience*. https://doi.org/10.1038/nrn3176

39. Erturk, A., Hellal, F., Enes, J., & Bradke, F. (**2007**). Disorganized Microtubules Underlie the Formation of Retraction Bulbs and the Failure of Axonal Regeneration. *Journal of Neuroscience*, 27(34), 9169–9180. https://doi.org/10.1523/JNEUROSCI.0612-07.2007

40. Tom, V. J., Steinmetz, M. P., Miller, J.H., Doller, C. M., Silver, J. (**2004**). Studies on the development and behavior of the dystrophic growth cone, the hallmark of regeneration failure, in an in vitro model of the glial scar and after spinal cord injury. *Journal of Neuroscience*, 24(29), 6531-6539. https://doi.org/10.1523/JNEUROSCI.0994-04.2004

41. Ruschel, J., Hellal, F., Flynn, K. C., Dupraz, S., Elliot, D. A., Tedeschi, A., Bradke, F. (**2015**). Systemic Administration of Epothilone B Promotes Axon Regeneration and Functional Recovery after Spinal Cord Injury. *Science*, 348(6232), 347–352. https://doi.org/10.1038/ja.2013.113.Venturicidin

42. Hellal, F., Hurtado, A., Ruschel, J., Flynn, K., Umlauf, M., Strikis, D., Hoogenraad, C. (**2012**). Microtubule stabilization reduces scarring and enables axon regeneration after spinal cord injury. *Science*, 331(6019), 928–931. https://doi.org/10.1126/science.1201148.Microtubule

43. Sengottuvel, V., Leibinger, M., Pfreimer, M., Andreadaki, A., Fischer, D. (**2011**). Taxol facilitates axon regeneration in the mature CNS. *Journal of Neuroscience*, 31(7), 2688-2699. https://doi.org/10.1523/JNEUROSCI.4885-10.2011

44. Ben-Yaakov, K., Dagan, S. Y., Segal-Ruder, Y., Shalem, O., Vuppalanchi, D., Willis, D. E., Fainzilber, M. (**2012**). Axonal transcription factors signal retrogradely in lesioned peripheral nerve. *EMBO Journal*, 31(6), 1350–1363. https://doi.org/10.1038/emboj.2011.494

45. Hanz, S., Perlson, E., Willis, D., Zheng, J. Q., Massarwa, R., Huerta, J. J., Fainzilber, M. (**2003**). Axoplasmic importins enable retrograde injury signaling in lesioned nerve. *Neuron*, 40(6), 1095–1104. https://doi.org/10.1016/S0896-6273(03)00770-0

46. Mar, F. M., Simoes, A. R., Leite, S., Morgado, M. M., Santos, T. E., Rodrigo, I. S., Sousa, M. M. (**2014**). CNS Axons Globally Increase Axonal Transport after Peripheral Conditioning. *Journal of Neuroscience*, 34(17), 5965–5970. https://doi.org/10.1523/JNEUROSCI.4680-13.2014

47. Nawabi, H., Belin, S., Cartoni, R., Williams, P. R., Wang, C., Latremolière, A., … He, Z. (**2015**). Doublecortin-Like Kinases Promote Neuronal Survival and Induce Growth Cone Reformation via Distinct Mechanisms. *Neuron*, 88(4), 704–719. https://doi.org/10.1016/j.neuron.2015.10.005

48. Ruschel, J., & Bradke, F. (**2017**). Systemic administration of epothilone D improves functional recovery of walking after rat spinal cord contusion injury. *Experimental Neurology*. https://doi.org/10.1016/j.expneurol.2017.12.001

49. Hammond, J. W., Cai, D., & Verhey, K. J. (**2008**). Tubulin modifications and their cellular functions. *Current Opinion in Cell Biology*. https://doi.org/10.1016/j.ceb.2007.11.010

50. Janke, C., & Bulinski, J. C. (**2011**). Post-translational regulation of the microtubule cytoskeleton: Mechanisms and functions. *Nature Reviews Molecular Cell Biology*. https://doi.org/10.1038/nrm3227

51. L'Hernault, S. W., & Rosenbaum, J. L. (**1985**). Chlamydomonas alpha-tubulin is posttranslationally modified by acetylation on the epsilon-amino group of a lysine. *Biochemistry*, 24(2), 473–478. https://doi.org/10.1021/bi00323a034

52. Maruta, H., Greer, K., & Rosenbaum, J. L. (**1986**). The acetylation of alpha-tubulin and its relationship to the assembly and disassembly of microtubules. *Journal of Cell Biology*, 103(2), 571–579. https://doi.org/10.1083/jcb.103.2.571

53. Hubbert, C., Guardiola, A., Shao, R., Kawaguchi, Y., Ito, A., Nixon, A., Yao, T. P. (**2002**). HDAC6 is a microtubule-associated deacetylase. *Nature*, 417(6887), 455–458. https://doi.org/10.1038/417455a

54. North, B. J., Marshall, B. L., Borra, M. T., Denu, J. M., & Verdin, E. (**2003**). The human Sir2 ortholog, SIRT2, is an NAD+-dependent tubulin deacetylase. *Molecular Cell*, 11(2), 437–444. https://doi.org/10.1016/S1097-2765(03)00038-8

55. LeDizet, M., & Piperno, G. (**1986**). Cytoplasmic microtubules containing acetylated α-tubulin in Chlamydomonas reinhardtii: Spatial arrangement and properties. *The Journal of Cell Biology*, 103(1), 13–22. https://doi.org/10.1083/jcb.103.1.13

56. Piperno, G., LeDizet, M., & Chang, X. J. (**1987**). Microtubules containing acetylated alpha-tubulin in mammalian cells in culture. *The Journal of Cell Biology*, 104(2), 289–302. https://doi.org/10.1083/jcb.104.2.289

57. Zhang, L., Liu, C., Wu, J., Tao, J. J., Sui, X. L., Yao, Z. G., Qin, C. (**2014**). Tubastatin A/ACY-1215 improves cognition in Alzheimer's disease transgenic mice. *Journal of Alzheimer's Disease*, 41(4), 1193–1205. https://doi.org/10.3233/JAD-140066

58. Cartelli, D., Casagrande, F., Busceti, C. L., Bucci, D., Molinaro, G., Traficante, A., Cappelletti, G. (**2013**). Microtubule alterations occur early in experimental parkinsonism and the microtubule stabilizer Epothilone D is neuroprotective. *Scientific Reports*, 3. https://doi.org/10.1038/srep01837

59. Dompierre, J. P., Godin, J. D., Charrin, B. C., Cordelieres, F. P., King, S. J., Humbert, S., & Saudou, F. (**2007**). Histone Deacetylase 6 Inhibition Compensates for the Transport Deficit in Huntington's Disease by Increasing Tubulin Acetylation. *Journal of Neuroscience*, 27(13), 3571–3583. https://doi.org/10.1523/JNEUROSCI.0037-07.2007

60. D'Ydewalle, C., Krishnan, J., Chiheb, D. M., Van Damme, P., Irobi, J., Kozikowski, A. P., Van Den Bosch, L. (**2011**). HDAC6 inhibitors reverse axonal loss in a mouse model of mutant HSPB1-induced Charcot-Marie-Tooth disease. *Nature Medicine*, 17(8), 968–974. https://doi.org/10.1038/nm.2396

61. Zou, H., Wu, Y., Navre, M., & Sang, B. C. (**2006**). Characterization of the two catalytic domains in histone deacetylase 6. *Biochemical and Biophysical Research Communications*, 341(1), 45–50. https://doi.org/10.1016/j.bbrc.2005.12.144

62. Zilberman, Y., Ballestrem, C., Carramusa, L., Mazitschek, R., Khochbin, S., & Bershadsky, A. (**2009**). Regulation of microtubule dynamics by inhibition of the tubulin deacetylase HDAC6. *Journal of Cell Science,* 122(19), 3531-3541. https://doi.org/10.1242/jcs.046813

63. Rivieccio, M. A., Brochier, C., Willis, D. E., Walker, B. A., D'Annibale, M. A., McLaughlin, K., Langley, B. (**2009**). HDAC6 is a target for protection and regeneration following injury in the nervous system. *Proceedings of the National*

Academy of Sciences, 106(46), 19599–19604. https://doi.org/10.1073/pnas.0907935106

64. Jochems, J., Boulden, J., Lee, B. G., Blendy, J. A., Jarpe, M., Mazitschek, R., Berton, O. (**2014**). Antidepressant-like properties of novel HDAC6-selective inhibitors with improved brain bioavailability. *Neuropsychopharmacology*, 39(2), 389–400. https://doi.org/10.1038/npp.2013.207

65. Majid, T., Griffin, D., Criss, Z., Jarpe, M., & Pautler, R. G. (**2015**). Pharmocologic treatment with histone deacetylase 6 inhibitor (ACY-738) recovers Alzheimer's disease phenotype in amyloid precursor protein/presenilin 1 (APP/PS1) mice. *Alzheimer's and Dementia: Translational Research and Clinical Interventions*, 1(3), 170–181. https://doi.org/10.1016/j.trci.2015.08.001

66. Regna, N. L., Vieson, M. D., Luo, X. M., Chafin, C. B., Puthiyaveetil, A. G., Hammond, S. E., … Reilly, C. M. (**2016**). Specific HDAC6 inhibition by ACY-738 reduces SLE pathogenesis in NZB/W mice. *Clinical Immunology*, 162, 58–73. https://doi.org/10.1016/j.clim.2015.11.007

67. Van Helleputte, L., Kater, M., Cook, D. P., Eykens, C., Rossaert, E., Haeck, W., Van Den Bosch, L. (**2018**). Inhibition of histone deacetylase 6 (HDAC6) protects against vincristine-induced peripheral neuropathies and inhibits tumor growth. *Neurobiology of Disease*, 111, 59–69. https://doi.org/10.1016/j.nbd.2017.11.011

68. Sroga, J. M., Jones, T. B., Kigerl, K. A., McGaughy, V. M., & Popovich, P. G. (**2003**). Rats and mice exhibit distinct inflammatory reactions after spinal cord injury. *The Journal of Comparative Neurology*, 462(2), 223–240. https://doi.org/10.1002/cne.10736

69. Suzuki, K., Suzuki, K. (**1983**). The twitcher mouse. A model of human globoid cell leukodystrophy (Krabbe's disease). *The American Journal of Pathology,* 111(3), 394–397. PubMed PMID: 6859223

70. Suzuki, K., Suzuki, Y. (**1970**). Globoid Cell Leucodystrophy (Krabbe's Disease): Deficiency of Galactocerebroside -Galactosidase. *Proceedings of the National Academy of Sciences*, 66(2), 302–309. https://doi.org/10.1073/pnas.66.2.302

71. Suzuki, Y., Suzuki, K. (**1971**). Krabbe's globoid cell leukodystrophy: deficiency of galactocerebrosidase in serum, leukocytes, and fibroblasts. *Science*, 171, 73-75. https://doi.org/ 10.1126/science.171.3966.73

72. Suzuki, K. (**2003**). Evolving perspective of the pathogenesis of globoid cell leukodystrophy (Krabbe disease). *Proceedings of the Japan Academy, Series B*, 79B(1), 1-8. https://doi.org/10.2183/pjab.79B.1

73. Suzuki, K. (**2003**). Globoid cell leukodystrophy (Krabbe's disease): Update. *Journal of Child Neurology*, 18(9), 595–603. https://doi.org/10.1177/08830738030180090201

74. Suzuki K., Tanaka H., Suzuki K. (**1976**) Studies on the Pathogenesis of Krabbe's Leukodystrophy: Cellular Reaction of the Brain to Exogenous Galactosylsphingosine, Monogalactosyl Diglyceride, and Lactosylceramide. In: Volk B.W., Schneck L. (eds) *Current Trends in Sphingolipidoses and Allied Disorders. Advances in Experimental Medicine and Biology*, vol 68. Springer, Boston, MA, pp 99-114

75. Duchen, L.W., Eicher, E.M., Jacobs, J.M., Scaravilli, F., Teixeira, F. (**1980**). Hereditary leucodystrophy in the mouse: the new mutant twitcher. *Brain*, 103(3), 695-710. https://doi.org/10.1093/brain/103.3.695

76. Kobayashi, T., Yamanaka, T., Jacobs, J. M., Teixeira, F., & Suzuki, K. (**1980**). The twitcher mouse: an enzymatically authentic model of human globoid cell leukodystrophy (Krabbe disease). *Brain Research*. https://doi.org/10.1016/0006-8993(80)90159-6

77. Sakai, N., Inui, K., Tatsumi, N., Fukushima, H., Nishigaki, T., Taniike, M., Ozono, K. (**1996**). Molecular Cloning and Expression of eDNA for Murine Galactocerebrosidase and Mutation Analysis of the Twitcher Mouse, a Model of Krabbe's Disease. *Journal of Neurochemistry*, 66(3), 1118–1124. PubMed PMID: 8769874

78. De Gasperi, R., Friedrich, V. L., Perez, G. M., Senturk, E., Wen, P. H., Kelley, K., Gama Sosa, M. A. (**2004**). Transgenic rescue of Krabbe disease in the twitcher mouse. *Gene Therapy*, 11(15), 1188–1194. https://doi.org/10.1038/sj.gt.3302282

79. Teixeira, C. A., Miranda, C. O., Sousa, V. F., Santos, T. E., Malheiro, A. R., Solomon, M., … Sousa, M. M. (**2014**). Early axonal loss accompanied by impaired endocytosis, abnormal axonal transport, and decreased microtubule stability occur in the model of Krabbe's disease. *Neurobiology of Disease*, 66, 92–103. https://doi.org/10.1016/j.nbd.2014.02.012

80. Schmitz, S. K., Hjorth, J. J. J., Joemai, R. M. S., Wijntjes, R., Eijgenraam, S., Bruijn, P. De, … Veldkamp, W. (**2011**). Automated analysis of neuronal morphology, synapse number and synaptic recruitment. *Journal of Neuroscience Methods*, 195(2), 185–193. https://doi.org/10.1016/j.jneumeth.2010.12.011

81. Wong, V. S. C., Picci, C., Swift, M., Levinson, M., Willis, D., & Mag, C. (**2018**). α–Tubulin Acetyltransferase Is a Novel Target Mediating Neurite Growth Inhibitory Effects of Chondroitin Sulfate Proteoglycans and Myelin- Associated Glycoprotein. *ENeuro*, 5(1), 1–13. https://doi.org/10.1523/ENEURO.0240-17.2018

82. Brockes, J. F., & Kumar, A. (**2005**). Appendage regeneration in adult vertebrates and implications for regenerative medicine. *Science*. https://doi.org/10.1126/science.1115200

83. Poss, K. D. (**2010**). Advances in understanding tissue regenerative capacity and mechanisms in animals. *Nature Reviews Genetics*. https://doi.org/10.1038/nrg2879

84. Mokalled, M. H., Patra, C., Dickson, A. L., Endo, T., Stainier, D. Y. R., & Poss, K. D. (**2016**). Injury-induced ctgfa directs glial bridging and spinal cord regeneration in zebrafish. *Science*, 354(6312), 630–634. https://doi.org/10.1126/science.aaf2679

85. Tanaka, E. M. (**2003**). Cell differentiation and cell fate during urodele tail and limb regeneration. *Current Opinion in Genetics & Development*, 13(5), 497–501. https://doi.org/10.1016/j.gde.2003.08.003

86. Kragl, M., Knapp, D., Nacu, E., Khattak, S., Maden, M., Epperlein, H. H., & Tanaka, E. M. (**2009**). Cells keep a memory of their tissue origin during axolotl limb regeneration. *Nature*. https://doi.org/10.1038/nature08152

87. Brunjes, P. C. (**1990**). The precocial mouse, Acomys cahirinus. *Psychobiology*, 18(3), 339–350. https://doi.org/10.3758/BF03327252

88. Chevret, P., Denys, C., Jaeger, J. J., Michaux, J., & Catzeflis, F. M. (**1993**). Molecular evidence that the spiny mouse (Acomys) is more closely related to gerbils (Gerbillinae) than to true mice (Murinae). *Proceedings of the National Academy of Sciences*, 90(8), 3433–3436. https://doi.org/10.1073/pnas.90.8.3433

89. Haughton, C. L., Gawriluk, T. R., & Seifert, A. W. (**2016**). The Biology and Husbandry of the African Spiny Mouse (Acomys cahirinus) and the Research Uses of a Laboratory Colony. *Journal of the American Association for Laboratory Animal Science: JAALAS*, 55(1), 9–17. Retrieved from http://www.ncbi.nlm.nih.gov/pubmed/26817973

90. Seifert, A. W., Kiama, S. G., Seifert, M. G., Goheen, J. R., Palmer, T. M., & Maden, M. (**2012**). Skin shedding and tissue regeneration in African spiny mice (Acomys). *Nature*, 489(7417), 561–565. https://doi.org/10.1038/nature11499

91. Matias Santos, D., Rita, A. M., Casanellas, I., Brito Ova, A., Araújo, I. M., Power, D., & Tiscornia, G. (**2016**). Ear wound regeneration in the African spiny mouse Acomys cahirinus. *Regeneration*, 3(1), 52–61. https://doi.org/10.1002/reg2.50

92. Gawriluk, T. R., Simkin, J., Thompson, K. L., Biswas, S. K., Clare-Salzler, Z., Kimani, J. M., … Seifert, A. W. (**2016**). Comparative analysis of ear-hole closure

identifies epimorphic regeneration as a discrete trait in mammals. *Nature Communications*, 7, 1–16. https://doi.org/10.1038/ncomms11164

93. Xue, M., & Jackson, C. J. (**2015**). Extracellular Matrix Reorganization During Wound Healing and Its Impact on Abnormal Scarring. *Advances in Wound Care*, 4(3), 119–136. https://doi.org/10.1089/wound.2013.0485

94. Brant, J. O., Lopez, M.-C., Baker, H. V, Barbazuk, W. B., & Maden, M. (**2015**). A Comparative Analysis of Gene Expression Profiles during Skin Regeneration in Mus and Acomys. *PloS One*, 10(11), e0142931. https://doi.org/10.1371/journal.pone.0142931

95. Hara, M., Kobayakawa, K., Ohkawa, Y., Kumamaru, H., Yokota, K., Saito, T., Okada, S. (**2017**). Interaction of reactive astrocytes with type i collagen induces astrocytic scar formation through the integrin-N-cadherin pathway after spinal cord injury. *Nature Medicine*, 23(7), 818–828. https://doi.org/10.1038/nm.4354

96. Tonge, D. A., De Burgh, H. T., Docherty, R., Humphries, M. J., Craig, S. E., & Pizzey, J. (**2012**). Fibronectin supports neurite outgrowth and axonal regeneration of adult brain neurons in vitro. *Brain Research*, 1453, 8–16. https://doi.org/10.1016/j.brainres.2012.03.024

97. King, V. R., Alovskaya, A., Wei, D. Y. T., Brown, R. A., & Priestley, J. V. (**2010**). The use of injectable forms of fibrin and fibronectin to support axonal ingrowth after spinal cord injury. *Biomaterials*, 31(15), 4447–4456. https://doi.org/10.1016/j.biomaterials.2010.02.018

98. King, V. R., Henseler, M., Brown, R. A., & Priestley, J. V. (**2003**). Mats made from fibronectin support oriented growth of axons in the damaged spinal cord of the adult rat. *Experimental Neurology*, 182(2), 383–398. https://doi.org/10.1016/S0014-4886(03)00033-5

99. Lochter, a, & Schachner, M. (**1993**). Tenascin and extracellular matrix glycoproteins: from promotion to polarization of neurite growth in vitro. *The Journal of Neuroscience: The Official Journal of the Society for Neuroscience*, 13(September), 3986–4000.

100. Chen, J., Joon Lee, H., Jakovcevski, I., Shah, R., Bhagat, N., Loers, G., Schachner, M. (**2010**). The extracellular matrix glycoprotein tenascin-c is beneficial for spinal cord regeneration. *Molecular Therapy*, 18(10), 1769–1777. https://doi.org/10.1038/mt.2010.133

101. Brant, J. O., Yoon, J. H., Polvadore, T., Barbazuk, W. B., & Maden, M. (**2016**). Cellular events during scar-free skin regeneration in the spiny mouse, Acomys. *Wound Repair and Regeneration*, 24(1), 75–88. https://doi.org/10.1111/wrr.12385

102. Zhu, Y., Soderblom, C., Krishnan, V., Ashbaugh, J., Bethea, J. R., & Lee, J. K. (**2015**). Hematogenous macrophage depletion reduces the fibrotic scar and increases axonal growth after spinal cord injury. *Neurobiology of Disease*, 74, 114–125. https://doi.org/10.1016/j.nbd.2014.10.024

103. Petrie, T. A., Strand, N. S., Yang, C.-T., Rabinowitz, J. S., & Moon, R. T. (**2015**). Macrophages modulate adult zebrafish tail fin regeneration. *Development*, 142(2), 406–406. https://doi.org/10.1242/dev.120642

104. Godwin, J. W., Pinto, A. R., & Rosenthal, N. A. (**2013**). Macrophages are required for adult salamander limb regeneration. *Proceedings of the National Academy of Sciences*, 110(23), 9415–9420. https://doi.org/10.1073/pnas.1300290110

105. Simkin, J., Gawriluk, T. R., Gensel, J. C., & Seifert, A. W. (**2017**). Macrophages are necessary for epimorphic regeneration in African spiny mice. *ELife*, 6. https://doi.org/10.7554/eLife.24623

106. Yun, M. H., Davaapil, H., & Brockes, J. P. (**2015**). Recurrent turnover of senescent cells during regeneration of a complex structure. *ELife*, 4. https://doi.org/10.7554/eLife.05505

107. Basso, D. M., Fisher, L. C., Anderson, A. J., Jakeman, L. B., Mctigue, D. M., & Popovich, P. G. (**2006**). Basso Mouse Scale for Locomotion Detects Differences in Recovery after Spinal Cord Injury in Five Common Mouse Strains. *Journal of Neurotrauma*, 23(5), 635–659. https://doi.org/10.1089/neu.2006.23.635

108. Ghosh, M., & Pearse, D. D. (**2014**). The role of the serotonergic system in locomotor recovery after spinal cord injury. *Frontiers in Neural Circuits*, 8, 151. http://doi.org/10.3389/fncir.2014.00151

109. Katsetos, C.D., Herman, M.M., Mörk, S.J. (**2003**). Class III beta-tubulin in human development and cancer. *Cell Motility and the Cytoskeleton*, 55(2), 77-96. https://doi.org/10.1002/cm.10116

110. Shin, J.E., Geisler, S., DiAntonio, A. (**2014**). Dynamic regulation of SCG10 in regenerating axons after injury. *Experimental Neurology*, 252, 1-11. https://doi.org/10.1016/j.expneurol.2013.11.007

111. Ito, D., Imai, Y., Ohsawa, K., Nakajima, K., Fukuuchi, Y., Kohsaka, S. (**1998**). Microglia-specific localisation of a novel calcium binding protein, Iba1. *Brain Research. Molecular Brain Research,* 57(1), 1-9. https://doi.org/10.1016/S0169-328X(98)00040-0

112. Austyn, J.M., Gordon, S. (**1981**). F4/80, a monoclonal antibody directed specifically against the mouse macrophage. *European Journal of Immunology*, 11(10), 805-815. https://doi.org/10.1002/eji.1830111013

113. Betjes, M.G., Haks, M.C., Tuk, C.W., Beeleen, R.H. (**1991**). Monoclonal antibody EBM11 (anti-CD68) discriminates between dendritic cells and macrophages after short-term culture. *Immunobiology*, 183(1-2), 79-87. https://doi.org/10.1016/S0171-2985(11)80187-7

114. Chen, H., Zhang, L., Hill, W.G., Yu, W. (**2017**). Evaluating the voiding spot assay in mice: a simple method with complex environmental interactions. *American Journal of Physiology. Renal Physiology,* 313(6), 1274-1280. https://doi.org/10.1152/ajprenal.00318.2017

115. Hughes, J. T. (**1988**). The Edwin Smith surgical papyrus: An analysis of the first case reports of spinal cord injuries. *Paraplegia*, 26(2), 71–82. https://doi.org/10.1038/sc.1988.15